Biochem. J. (2014) **462**, 567–579 (Printed in Great Britain) doi:10.1042/BJ20140577

Regulation of PKA activity by an autophosphorylation mechanism in *Saccharomyces cerevisiae*

Clara Andrea SOLARI*, Vanesa TUDISCA*, Marcelo PUGLIESSI*, Alejandro Daniel NADRA*, Silvia MORENO* and Paula PORTELA*[1]

*Instituto de Química Biológica, Facultad de Ciencias Exactas y Naturales (IQUIBICEN-CONICET), Universidad de Buenos Aires, Buenos Aires, Argentina

PKA (cAMP-dependent protein kinase) activity, as well as that of other AGC members, is regulated by multiple phosphorylations of its catalytic subunits. In *Saccharomyces cerevisiae*, the PKA regulatory subunit is encoded by the gene *BCY1*, and the catalytic subunits are encoded by three genes: *TPK1*, *TPK2* and *TPK3*. Previously, we have reported that, following cAMP/PKA pathway activation, Tpk1 increases its phosphorylation status. Now, *in vivo* genetic and *in vitro* experiments indicate an autophosphorylation mechanism for Tpk1. Using array peptides derived from Tpk1, we identified Ser^{179} as a target residue. Tpk1 is phosphorylated on Ser^{179} *in vivo* during glucose stimulus. Reduction of the activation loop Thr^{241} phosphorylation increases Ser^{179} autophosphorylation. To evaluate the role of phosphorylation on Ser^{179}, we made strains expressing *tpk1*^{S179A} or *tpk1*^{S179D} as the sole PKA kinase source. Our results suggest that Ser^{179} phosphorylation increases the reactivity towards the substrate without affecting the formation of the holoenzyme. Phenotypic readout analysis showed that Ser^{179} phosphorylation increases *in vivo* PKA activity, reducing cell survival, stress and lifespan. Ser^{179} phosphorylation increases Tpk1 cytoplasmic accumulation in glucose-grown cells. These results describe for the first time that an autophosphorylation mechanism on Tpk1 controls PKA activity in response to glucose availability.

Key words: cAMP-dependent protein kinase (PKA), phosphorylation, *Saccharomyces cerevisiae*, Tpk1.

INTRODUCTION

Protein kinases have a conserved kinase core which is regulated by tails and linker segments which can differ in each kinase. Post-translational modifications, such as phosphorylation, can modulate the entire structure and function of a kinase protein. Phosphorylation can operate as an electrostatic switch or regulate protein–protein interactions affecting macromolecular signalling complex assembly [1]. Within the AGC family of protein kinases, PKA (cAMP-dependent protein kinase) has been studied extensively. The mammalian catalytic subunit of PKA is assembled by two distinct phosphorylation events: an initial intramolecular co-translational autophosphorylation of Ser^{338} in the C-terminal tail, followed by an intermolecular post-translational phosphorylation of Thr^{197} in the activation loop [2]. Phosphorylated catalytic subunits bound to either type I or II regulatory subunits, and therefore are maintained in an inactive conformation. There is no direct evidence indicating whether Thr^{197} phosphorylation occurs via autophosphorylation or via PDK1 (3-phosphoinositide-dependent protein kinase 1)-mediated phosphorylation [3,4].

In *Saccharomyces cerevisiae*, PKA is a heterotetramer formed by two regulatory (R) subunits (encoded by the *BCY1* gene) and two catalytic (C) subunits (encoded by three partially redundant *TPK1*, *TPK2* and *TPK3* genes). Recently, it has been shown that Pkh1 (homologue of mammalian PDK1) phosphorylates the activation loop of Tpk1 (Thr^{241}) *in vitro*, and Pkh1–Pkh3 are required for *in vivo* Thr^{241} phosphorylation in newly synthesized Tpk1 [5]. Lack of Thr^{241} phosphorylation reduces the interaction of Tpk1 catalytic subunit with the regulatory subunit Bcy1 without affecting PKA specific activity [6].

In *S. cerevisiae*, PKA signalling plays a key role in the nutrient response. In yeast growing on a non-fermentable carbon source (non-repressed cells) such as glycerol or acetate, the addition of glucose triggers a rapid and transient increase in cAMP levels, initiating a phosphorylation cascade mediated by PKA [7]. Glucose addition activates adenylate cyclase through two different G-protein systems: Gpr1/Gpa2/Rgs2 GPCR (G-protein-coupled receptor) system which senses extracellular glucose and the Cdc25/Sdc25-Ras1/2-Ira1/Ira2 system that senses intracellular glucose through glucose catabolism in glycolysis [8]. The Krh1/Krh2 kelch repeat proteins mediate a cAMP-independent pathway triggered by the glucose-sensing GPCR system. Krh1/Krh2 bind directly to Tpk subunits, thereby stimulating Tpk–Bcy1 association [9,10]. Upon glucose limitation, Krh1/Krh2 bind Bcy1, protecting it from PKA phosphorylation and consequent protein degradation [11,12]. PKA itself contributes to the negative-feedback loop on cAMP levels by regulating the activity, protein abundance and localization of low- and high-affinity phosphodiesterases (Pde1 and Pde2 respectively) [13,14].

Besides glucose, different essential nutrients can trigger rapid activation of the PKA pathway, such as the amino acid addition to nitrogen-deprived cells, through a mechanism not associated with an increase in cAMP [15,16]. This pathway is involved in the maintenance of fermentative metabolism and requires a

Abbreviations: CLS, chronological lifespan; GPCR, G-protein-coupled receptor; HA, haemagglutinin; PDK1, 3-phosphoinositide-dependent protein kinase 1; PKA, cAMP-dependent protein kinase; Pkh1, homologue of mammalian PDK1; PKI, protein kinase inhibitor; SD, synthetic dropout; TAP, tandem affinity purification; TCA, tricholoroacetic acid.

[1] To whom correspondence should be addressed (email pportela@qb.fcen.uba.ar).

fermentable carbon source and a complete growth medium for its sustained activation, it is known as the 'FGM (fermentable growth medium)-induced pathway' [17].

Subcellular localization of PKA subunits is strongly regulated by nutrient availability and stress conditions. This provides an additional level of PKA activity regulation. In exponentially growing cells of glucose, Bcy1 and Tpk2 localization is mainly nuclear, whereas Tpk1 and Tpk3 show nucleocytoplasmic distribution [18]. The nuclear accumulation of Tpk1 seems to be dependent on its interaction with Bcy1 [18]. Inactivation of Sch9 protein kinase promotes Bcy1 nuclear accumulation and Tpk cytoplasmic localization, which results in a high-activity PKA phenotype [19]. Stationary phase or glucose-starved cells show relocalization of all PKA subunits towards the cytoplasm, where Tpk2 and Tpk3, in particular, are accumulated in RNP (ribonucleoprotein) granules [20,21].

We have reported previously that, concomitant with cAMP–PKA activation evoked by glucose addition on glycerol-growing cells, Tpk1 changes its phosphorylation status towards hyperphosphorylated isoforms. This process is dependent on cAMP levels and on PKA activation through the GPCR pathway. This change in the phosphorylation status of Tpk1 is fully dependent on the presence of an active version of Tpk1. As a consequence, Tpk1 increases its specific activity towards kemptide [22]. The precise phosphorylation site(s) target of Tpk1 phosphorylation as well as its molecular mechanism has not yet been studied. In the present study, we have elucidated the mechanism of glucose-evoked Tpk1 phosphorylation and identified one target residue as well as its role in the regulation of PKA activity. We describe for the first time an autophosphorylation mechanism of Tpk1 on Ser^{179} during the transition from respiratory to fermentative metabolism. Ser^{179} phosphorylation of Tpk1 promotes an increase in its kinase activity, contributing to fully sustain the fermentative metabolism. Our findings identify a novel mechanism of PKA activity control by phosphorylation of its catalytic subunit in response to nutrient availability.

EXPERIMENTAL

Yeast strains, plasmids, media and growth conditions

Yeast strains and plasmids used in the present study are described in Supplementary Tables S1 and S2 (http://www.biochemj.org/bj/462/bj4620567add.htm) respectively. Yeast strains were transformed using the lithium acetate method [23], and transformants were selected on SD (synthetic dropout) medium lacking the appropriate amino acid supplement.

The single-site mutants of Tpk1 in which Ser^{179} was replaced with an alanine or aspartate residue were obtained using conventional PCR-based methods, using complementary mutagenic oligonucleotide primers and pTD45-Tpk1 construct as the template (TOP Gene Technologies). All constructs were sequenced. Epitope tagging was constructed using the cellular repair machinery to incorporate the PCR fragment into a gapped plasmid via gap repair [24] or into the genomic locus [25]. A fragment containing the C-terminal coding region of the *TPK1* gene fused to a GFP or TAP (tandem affinity purification) epitope carrying the *HIS3* selectable marker was amplified by PCR from genomic DNA using the primers 5′-TTGTTAAGGAAAGCCCAAAGATTTCCCAAC-3′ (forward) and 5′-GATTCCGACCTTGTTTGGAGC-3′ (reverse). Fragment for epitope tagging of Bcy1 was generated using the primers 5′-AGACCATGATTATTTCGGTG-3′ (forward) and 5′-GTAGTAACAGCAGTAGTAGA-3′ (reverse) employing genomic DNA from SC288C Bcy1-GFP strain. The DNA sequence was confirmed by sequencing, and the expression of tagged protein was monitored by Western blotting.

Strains CS-S179, CS-S179A and CS-S179D were constructed by deletion of the *TPK2* gene. The strain W303 *tpk3::tpk1::KanMx4* was transformed with pTD45-Tpk1, pTD45-$tpk1^{S179A}$ or pTD45-$tpk1^{S179D}$. A deletion cassette, generated by PCR, containing the *URA3* gene from *S. cerevisiae* flanked by a 50-bp region of the *TPK2* gene was transformed into each of these yeast strains. Transformants were selected on plates without uracil. Deletions in each strain were verified by PCR.

Strains were grown in rich medium containing 2 % (w/v) Bacto peptone, 1 % (w/v) yeast extract and 2 % (w/v) glycerol (YPGly), 2 % galactose (YPGal), 2 % glucose (YPGlu) or 2 % ethanol at 30 °C. Synthetic medium contained 0.67 % yeast nitrogen base without amino acids, 5 % ammonium sulfate and 2 % glucose (SDGlu) or 2 % glycerol (SDGly), plus the necessary additions to fulfil auxotrophic requirements and to maintain selectable plasmids. Solid medium contained 2 % agar. Carbon source-derepressed cells were grown on SDGly to exponential phase as indicated. Cells were collected by centrifugation at 4 °C, washed once with ice-cold 25 mM Mes/KOH (pH 6) and incubated for 15 min in fresh YPGly, before glucose (100 mM final concentration) addition. Aliquots were taken at different times and processed according to each determination. The zero time point always corresponds to samples taken immediately before glucose addition.

SDS/PAGE, native gel electrophoresis, 2D-gel electrophoresis and Western blotting

Samples of purified preparations or crude extracts were separated by SDS/PAGE (10 % gels). For native gel electrophoresis, the pelleted cells were disrupted in an appropriate buffer with glass beads and the lysate was clarified and mixed with native sample buffer (0.015 M Tris/HCl, pH 9, 5 % glycerol and 0.0125 % Bromophenol Blue). Gels were prepared essentially as described for SDS/PAGE, but SDS was omitted and the upper buffer was prepared with 0.15 M Tris/HCl (pH 9) [22]. For two-dimensional gel electrophoresis, a crude extract of $tpk1^{w1}$ + GFP–HA_3–Tpk1 strain was mixed with an equal volume of 20 % (v/v) TCA (tricholoroacetic acid) in acetone with 20 mM DTT and incubated for 45 min at − 20 °C before centrifugation for 15 min at 15000 ***g*** at 4 °C. The pellet was washed with ice-cold acetone with 20 mM DTT, incubated for 1 h at − 20 °C, centrifuged, dried and finally solubilized in lysis solution (50 μl/mg of dried pellet) for 2–4 h. The lysis solution contained 8 M urea, 2 % (w/v) Nonidet P40, 20 mM DTT, 0.01 % Bromophenol Blue and 0.5 % IPG buffer (GE Healthcare). The samples were used immediately or stored at − 80 °C until use. Protein samples of 125 μl (50 μg) were transferred into 7 cm IPG strips (pH 3–10) (GE Healthcare) for 15 h for rehydration. Isoelectric focusing was carried out at 20 °C with the Multiphor II system (GE Healthcare) at 500 V for 2 h, 1000 V for 2 h or 8000 V for 2 h. The strips were equilibrated in equilibration buffer (6 M urea, 20 mM DTT, 50 mM Tris/HCl, pH 8.8, 30 % glycerol, 2 % SDS and 0.01 % Bromophenol Blue) for 15 min, and subjected to second-dimension SDS/PAGE.

The gels were blotted on nitrocellulose membranes. Blots were probed with anti-TPK1, anti-BCY1, anti-HA (haemagglutinin), anti-GFP (Santa Cruz Biotechnology) or anti-$pSer^{179}$ phosphospecific polyclonal antibody. The anti-$pSer^{179}$ antibody was generated against the synthetic phosphopeptide CSLLRKpS^{179}QRFPNPVAK manufactured by Pacific Immunology. Anti-$pThr^{241}$ antibody was generously

provided by Professor Johan Thevelein [5]. The blots were developed with chemiluminescence luminol reagent, and immunoreactive bands were visualized by autoradiography and analysed by digital imaging using a Bio-Imaging Analyzer BAS-1800II (Fujifilm). To quantify Western blots, short exposures of two independent experiments were scanned and quantified using Image Gauge 3.12 software.

Purification of catalytic subunits and holoenzymes

Purification of HA-tagged proteins

Strains expressing HA-fused proteins were grown in SDGlu medium at the temperatures indicated in each Figure. Cells were subsequently lysed by disruption with glass beads using the appropriate buffer [26]. Cell debris was pelleted by centrifugation at 15000 ***g*** for 5 min, and the crude extract was used to immunoprecipitate HA-tagged proteins. The immunoprecipitation procedure was performed as described previously [26] using anti-HA antibody.

Purification of TAP-tagged proteins

Yeast cultures were grown to a D_{600} of 0.6. TAP-affinity purification was carried out on the cell lysates as described previously [27]. Holoenzyme purification was performed by one purification step: binding to IgG–Sepharose 4B through the Protein A IgG-binding domains of the ORF. This source of immobilized holoenzyme was used for PKA activation experiments. Catalytic subunit purification was performed following the holoenzyme protocol. After extensive washing of the immobilized holoenzymes on IgG–Sepharose 4B, the free catalytic subunits Tpk1, *tpk1*^{S179A} or *tpk1*^{S179D} were eluted with 50 mM cAMP. These sources of pure enzyme were immediately used for phosphorylation experiments as described below.

Kinase assay, holoenzyme activation and kinetic parameter determination

The kinase activity of purified Tpk1, *tpk1*^{S179A} and *tpk1*^{S179D} subunits were performed under standard assay conditions except for the Nth1-1 peptide GRQRRLSSLSEF used as substrate [28]. The reaction was started by mixing the samples with assay mixture. After 30 min at 30 °C, aliquots of 70 μl were processed using the phosphocellulose paper method [29]. Protein kinase assays were linear with time and kinase amount. Kinetic data were applied to the Michaelis–Menten equation. For the holoenzyme activation assays, immobilized purified PKA holoenzymes were used for measurement of kinase activity at various cAMP concentrations as described above using Nth1-1 substrate and calculating the $A_{0.5}$ value for cAMP under each condition.

Peptide array

The peptide array was designed by scanning all of the sequences in Tpk1 containing a serine or threonine, between 11 and 12 amino acids in length, with the phosphorylatable amino acid around the middle of the sequence. In cases where more than one phosphorylatable amino acid is present in the sequence, an additional version with a replacement of each one of the amino acids with alanine was included. Cellulose-bound peptide arrays were automatically prepared according to standard SPOT synthesis protocols by using a SPOT synthesizer (Abimed Analysentechnik) by Susan Taylor's laboratory, Department of Chemistry and Biochemistry, University of California at San Diego. The phosphorylation reaction was performed in an incubation mixture containing 0.2 mg/ml BSA, 100 μM ATP, 200 μCi of [γ-^{32}P]ATP and 150 pmol of Tpk1 subunits for 1 h at 30 °C [28]. The membrane was rinsed, dried and subjected to digital image analysis (Bio-Imaging Analyzer BAS-1800II and Image Gauge 3.12, Fujifilm).

In vitro Tpk1 phosphorylation reaction

Aliquots of 350 μl of purified Tpk1–TAP and *tpk1*^{d}–TAP fusion proteins were incubated in 400 μl of 50 mM Tris/HCl (pH 7.4), 10 mM NaCl, 1 mM DTT, 10 mM $MgCl_2$, 25 μM ATP, 45 μCi of [γ-^{32}P]ATP (4.5 Ci/mmol) (PerkinElmer Life Science) and 15 μg/ml PKI (protein kinase inhibitor) amide fragment 6–22, when added. The reaction was stopped after 30 min at 30 °C by precipitation with 25 % TCA. The samples were rehydrated with 20 μl of appropriate buffer plus 5 μl of Laemmli loading buffer (4×) and boiled for 5 min. The proteins were separated by SDS/PAGE (10 % gels). After silver staining, the gel was dried and exposed to X-ray film. To dephosphorylate the phosphorylated Tpk1–TAP protein, the ^{32}P-labelled Tpk1–TAP proteins were processed as described below.

Alkaline phosphatase treatment of catalytic subunit

Samples containing 80 μg of total protein or purified Tpk1 and *tpk1*^{d} samples were incubated at 37 °C for 15 min in a total volume of 40 μl with 0.1 M Tris/HCl (pH 9.5), 50 mM $MgCl_2$, 0.1 M NaCl and 100 units of alkaline phosphatase (Sigma). The reaction was stopped by the addition of phosphatase inhibitors. Samples treated with phosphatase or untreated samples were separated by native gel electrophoresis or SDS/PAGE.

Fluorescence microscopy

Cells used for fluorescence microscopy were grown to early exponential phase, fixed with 7.4 % formaldehyde, washed with PBS and resuspended in 0.05 % Nonidet P40 plus 1 μg/ml DAPI for 30 min to stain the nuclei. Microscopy was performed using an epifluorescence microscope (Nikon Eclipse E600W). The images were processed using ImageJ (NIH) and Adobe Photoshop CS2 software.

Phenotypes analysis

Glycogen accumulation was detected by the brown colour produced by staining with iodine, analysed *in situ* by inversion of a plate over I_2 crystals in a chromatography tank [30]. For heat-shock-resistance determination, yeast strains were pre-grown in appropriate medium until reaching 10^6 cells/ml. Heat shock was performed in a water bath at 56 °C for 8 min and cell viability was assayed by spot assay on SDGlu medium. CLS (chronological lifespan) was determined by measurement of cell viability of 12-old-day culture by spot assay on SDGlu [31]. Cell viability was assessed by spot assay and incubated for 48 h at 30 °C before photography. Glucose concentration in medium was determined using the Trinder method (Sigma).

Reproducibility of results

All experiments were repeated several times (indicated in each Figure) with independent cultures and enzyme preparations. Subcellular localization and glucose consumption was analysed

using ANOVA with Bonferroni's post-hoc test. Kinetic results were analysed using ANOVA with Tukey's HSD (honest significant difference) test.

RESULTS

Tpk1 changes its phosphorylation status by an autophosphorylation mechanism during the reconfiguration of respiratory to fermentative metabolism

Previously, we have shown that the phosphorylation status of Tpk1 changes towards more phosphorylated isoforms during the metabolic transition from respiratory to fermentative metabolism. The change in phosphorylation of Tpk1 occurs after a cAMP peak produced by glucose addition, and depends on the activation of cAMP/PKA pathway through a GPCR system. Furthermore, we did not observe changes in the phosphorylation status of Tpk1 when using an attenuated activity mutant *tpk1*^{w1}, suggesting that an active molecule is required for the increase in Tpk1 phosphorylation [22].

To analyse the mechanism responsible for this phosphorylation, we evaluated the phosphorylation state of Tpk1 during glucose stimulus on glycerol-growing cells using strains harbouring a chromosomally deleted *TPK1* gene, but expressing Tpk2 and Tpk3 (*tpk1*Δ *TPK2 TPK3 BCY1*) complemented with active Tpk1 or *tpk1*^{d} kinase-dead mutant (*tpk1*^{K116R}). We also the analysed phosphorylation status of Tpk1, employing strains harbouring a *tpk1*^{w1} weak kinase allele mutant (*tpk1*^{w1} *tpk2*Δ *tpk3*Δ *BCY1*) transformed with active versions of Tpk2 and Tpk3 isoforms. Tpk1 phosphorylation status before and after glucose addition was evaluated by native gel electrophoresis and Western blotting using anti-Tpk1 antibodies as described previously [22].

Immunoblot analysis (Figure 1A) of crude extracts from *tpk1*Δ + Tpk1 glycerol-growing cells ($t = 0$) showed two principal Tpk1 isoforms with a change in their relative abundance towards more phosphorylated isoforms 5 min after glucose stimulus ($t = 5$). Alkaline phosphatase treatment of samples of glucose-stimulated cells eliminated the faster-migrating isoforms, indicating that the modification in the migration pattern is due to phosphorylation ($t = 5$, − and + Ppase lanes). These results also confirm that Tpk1 from episomal expression has the same phosphorylation pattern as observed previously for Tpk1 expressed from genomic locus [22].

Interestingly, Tpk1 phosphorylation analysis in *tpk1*Δ + *tpk1*^{d} cells showed one principal isoform without any change upon glucose addition ($t = 0$ compared with $t = 5$). To verify the activation of the cAMP/PKA pathway in *tpk1*Δ + *tpk1*^{d} strain, we determined *in situ* PKA activity measured in permeabilized cells [22] and trehalose mobilization levels [32] on glycerol-growing cells stimulated by glucose (Figure 1C, upper panels). Upon glucose addition, both *tpk1*Δ + Tpk1 and *tpk1*Δ + *tpk1*^{d} strains showed a transient increase in endogenous PKA activity indicating cAMP/PKA pathway activation. Consistent with the absence of Tpk1 catalytic subunit, endogenous activation exerted by Tpk2 and Tpk3 isoforms during glucose stimulus reached half of PKA activity levels in a *tpk1*Δ + *tpk1*^{d} strain compared with a *tpk1*Δ + Tpk1 strain. The measurement of trehalose mobilization levels, as a readout of PKA activity (Figure 1C), showed a decrease in response to glucose addition, as expected.

Similarly to what we observed for the *tpk1*^{d} inactive version, the *tpk1*^{w1} attenuated mutant did not change its phosphorylation status upon glucose stimulus (Figure 1A). Additionally, *tpk1*^{w1} strain co-expressing a plasmid encoding either Tpk2 or Tpk3 isoforms did not increase *tpk1*^{w1} phosphorylation (Supplementary Figure S1 at http://www.biochemj.org/bj/462/bj4620567add.htm). Complementation with Tpk2 showed an increase in *in situ* PKA activity and glycogen and trehalose mobilization upon glucose stimulus, whereas complementation with Tpk3 showed reduced cAMP/PKA pathway activation possibly due to Tpk3 low expression (Supplementary Figure S1A). These results indicate that Tpk1 phosphorylation induced by glucose stimulation of the cAMP/PKA pathway is not exerted by Tpk2 or Tpk3 *trans*-phosphorylation.

To investigate whether Tpk1 phosphorylation is mediated by *trans*-phosphorylation between Tpk1 molecules, we employed strains co-expressing *tpk1*^{w1} and an active tagged version GFP–HA_3–Tpk1. Both versions of Tpk1 can be identified through their differential electrophoresis motilities. As shown in Figure 1(A), *tpk1*^{w1} did not change its phosphorylation status upon glucose addition when expressed alone or when co-expressed with the active version GFP–HA_3–Tpk1. The fusion protein GFP–HA_3–Tpk1 (denoted with asterisk in the anti-TPK1 blot and reblotted anti-HA membrane shown in Figure 1A) efficiently changed its phosphorylation pattern as observed when analysed via two-dimensional electrophoresis (Figure 1B). The phosphorylated isoforms of GFP–HA_3–Tpk1-tagged version were poorly resolved in native gels probably due to its increase in molecular mass. The cAMP/PKA activation in *tpk1*^{w1} strain complemented with GFP–HA_3–Tpk1 was verified through its transient increase in endogenous PKA activity and subsequent decline in trehalose levels induced by glucose addition to glycerol-growing cells (Figure 1C). Overall, these results suggest that *tpk1*^{w1} cannot be *trans*-phosphorylated by other Tpk1 molecules.

To analyse the catalytic activity requirement for Tpk1 phosphorylation *in vitro*, we performed a phosphorylation assay using a purified preparation of Tpk1 and [γ-^{32}P]ATP (Figure 2). The incorporation of ^{32}P into Tpk1 observed in the first lane of Figure 2 was abolished in the presence of PKI and reversed by alkaline phosphatase treatment (Figure 2, second and third lanes). Similar amounts of the purified kinase-dead version, *tpk1*^{d}, did not incorporate ^{32}P, indicating that only active Tpk1 molecules could be subjected to phosphorylation.

Identification of phosphorylation target site(s) in Tpk1

To identify the putative target residue(s) of autophosphorylation, we performed a peptide array screen. Taking into account our previous results that showed Tpk1 autophosphorylation, we synthesized a 10-mer peptide array containing all serine and threonine putative target residues from the Tpk1 protein sequence, with the phosphorylated amino acid centred in the sequence. To discriminate the target residue of phosphorylation, serine and threonine residues in peptides with more than one of these residues were replaced by alanine. Phosphorylation of kemptide peptide was used as positive control. The peptide array was incubated with purified Tpk1 plus [γ-^{32}P]ATP (Figure 3; see Supplementary Figure S2 at http://www.biochemj.org/bj/462/bj4620567add.htm for an image of the whole array). Figure 3(A) shows that the main phosphorylated peptide by far was L^{175}LRKSQRFPNP, containing Ser^{179}. To validate the results from the peptide array screen, we performed an *in vitro* kinase assay including peptides derived from negative spots and kemptide as positive control (Figure 3B). Three different sources of PKA were used, mammalian catalytic subunit (Cα), purified Tpk1 and permeabilized cells from *TPK1* *tpk2*Δ *tpk3*Δ *bcy1*Δ strain which has high and unregulated PKA activity. The L^{175}LRK**S**QRFPNP peptide was phosphorylated by the three PKA sources, suggesting that Ser^{179} (in bold) could be a target of Tpk1 autophosphorylation.

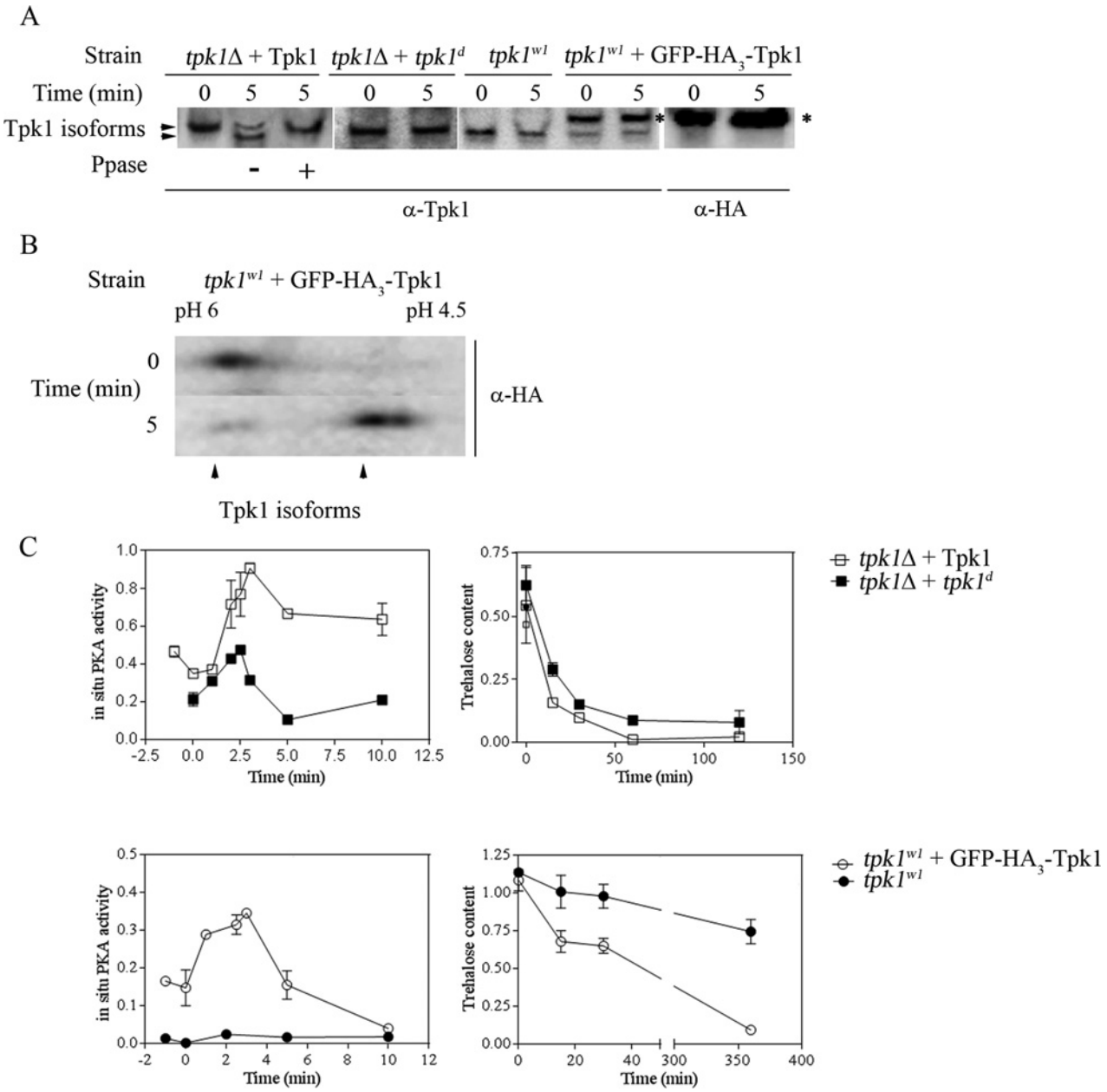

Figure 1 ***In vivo*** **phosphorylation of** ***tpk1*** **mutants evoked by glucose stimulus**

(**A**) Cells from *tpk1*Δ + Tpk1, *tpk1*Δ + *tpk1*^{d}, *tpk1*^{w1} and *tpk1*^{w1} + GFP–HA$_3$–Tpk1 strains were grown to exponential phase on SDGly. At time zero, 100 mM glucose was added. Samples were taken at time zero (before glucose addition) and at 5 min (after glucose addition). Equal amounts of protein from crude extracts were resolved by native gel electrophoresis and Tpk1 isoforms were detected using anti-Tpk1 or anti-HA antibody. An aliquot of the sample taken at 5 min from *tpk1*Δ + Tpk1 strain was treated with alkaline phosphatase (Ppase) before native gel electrophoresis. The fusion protein GFP–HA$_3$–Tpk1 is denoted with an asterisk in blot in the anti-TPK1 and the reblotted anti-HA membrane. (**B**) Aliquots from *tpk1*^{w1} + GFP–HA$_3$–Tpk1 strain were subjected to two-dimensional gel electrophoresis and the Tpk1–HA isoforms were developed using the anti-HA antibody. Arrowheads from left to right indicate lower and higher phosphorylated Tpk1. (**C**) *In situ* PKA activity measured in permeabilized cells (left-hand panels) and trehalose levels (right-hand panels) measured at variable times after 100 mM glucose addition to the cells. Results are means ± S.D. from three independent experiments.

It has been postulated that in order to evaluate the consequences of a phosphate group on a residue, mutation to alanine of residues corresponding to the consensus PKA site surrounding the target site is a better choice than mutating the phosphorylation site itself to alanine [2]. However, due to the fact that a catalytic subunit mutant *tpk1*^{R177A} or *tpk1*^{K178A} with mutations on either of the two consensus amino acids were defective in Tpk1–Bcy1 interaction [33], we chose the more classic approach and constructed a *TPK1* mutant in which Ser^{179} was replaced by alanine or aspartate. Before constructing the Tpk1 mutants, we evaluated the possible effects of a Ser^{179} mutation on the Tpk1 structure. Mutants were generated by FoldX 3.0 [34] which enables mutation to standard and phosphorylated residues and evaluation of changes in protein stability. We observed that Ser^{179} is situated at the end of the αD helix and that it is exposed to the solvent (Figure 3C). An available crystal structure of the catalytic subunit form *S.*

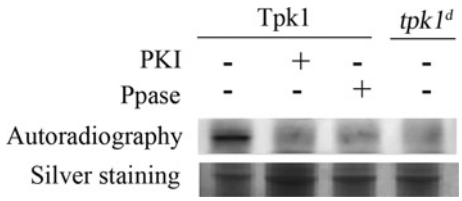

Figure 2 ***In vitro*** **phosphorylation of Tpk1 is dependent on an active catalytic subunit**

Equal amount of purified Tpk1–TAP and *tpk1*^{d}–TAP from glycerol-growing cells, were incubated with [γ-^{32}P]ATP for 30 min at 30 °C. PKI fragment peptide 6–22 was added to the phosphorylation reaction as indicated. An equivalent sample of ^{32}P-labelled Tpk1–TAP was incubated with alkaline phosphatase for 60 min at 30 °C. Samples were resolved by 10 % SDS/PAGE. Autoradiogram (upper panel) and silver staining (lower panel) of the same gel are shown.

cerevisiae (PDB code 1FOT) was used as a template to generate phosphorylated Ser^{179}, S179A and S179D mutants. All three mutants gave marginal destabilization values (within 0.3 kcal/mol; 1 kcal = 4.184 kJ), thus concluding that neither mutation nor phosphorylation significantly affects the protein stability.

Tpk1 phosphorylation on Ser^{179} occurs during the transition from respiratory to fermentative metabolism

To investigate whether Ser^{179} is a target residue of phosphorylation of Tpk1 *in vivo*, we employed phosphospecific antibodies developed against pSer^{179}. Specificity of anti-pSer^{179} antibody was verified by ELISA assay using synthetic phosphorylated and unphosphorylated peptides containing Ser^{179} (results not shown). We analysed the antibody specificity against Tpk1 proteins purified from cells grown in glucose; the antibody recognized purified wild-type Tpk1, but not the *tpk1*^{S179A} mutant version in which the serine residue was mutated to alanine (Figure 4A). Figure 4(B) shows that Tpk1 is phosphorylated on Ser^{179} during exponential growth on glucose, but its phosphorylation decreases significantly when cells are grown on glycerol or have reached stationary phase.

We next determined whether Tpk1 phosphorylation on Ser^{179} changes during PKA activation evoked by glucose stimulus on glycerol-growing cells. Exponentially growing cells on glycerol showed a low Ser^{179} phosphorylation, whereas glucose addition led to a rapid Ser^{179} phosphorylation within 5 min of stimulus (Figure 4C). At 90 min after stimulus, the degree of phosphorylation on Ser^{179} continued to be stable in levels similar to those observed in cells growing exponentially on glucose (Figure 4B, glucose lane). In cells expressing an attenuated Tpk1 version (*tpk1*^{w1}), phosphorylation of Ser^{179} after glucose stimulus was completely lost; even glycerol-growing cells showed no phosphorylation in this mutant weak version of Tpk1 (Figure 4C). These results indicate that Ser^{179} of Tpk1 is a target residue of glucose induced phosphorylation on active Tpk1 molecules.

It has been described that Tpk1 is phosphorylated by Pkh1 *in vivo* on the activation loop at Thr^{241} and its phosphorylation occurs during or immediately after Tpk1 synthesis. This phosphorylation was independent of nitrogen or glucose availability [5]. We have shown that Pkh1 inactivation reduces the interaction between Tpk1 and the regulatory subunit Bcy1 without affecting the specific kinase activity [6]. To assess the interrelationship between Thr^{241} and Ser^{179} phosphorylation, we first evaluated the phosphorylation state of Thr^{241} in Tpk1, *tpk1*^{S179A} and *tpk1*^{S179D} (Figure 4D, left-hand panel). Purified wild-type and mutant catalytic subunits from mid-exponential glucose cultures were subjected to Western blot analysis using anti-pThr^{241} antibody. Tpk1 protein showed similar levels of pThr^{241} signal independently of the presence of a negative charge on Ser^{179}, suggesting that the phosphorylation status of Ser^{179} did not affect the phosphorylation of Thr^{241} by Pkh1 kinase. Secondly, we analysed the phosphorylation state of Ser^{179} in a *pkh1*^{ts} *pkh2*Δ *pkh3*Δ strain (Figure 4D, right-hand panel) in which we have already shown that pThr^{241} is decreased [6]. We found an increased pSer^{179} signal in Tpk1 purified from the Pkh1 inactive strain. Consistent with previous data, this strain presents a reduced level of pThr^{241} and a decrease in the interaction between Tpk1 and Bcy1.

Collectively, these results indicate that a reduced phosphorylation state of Tpk1 on Thr^{241} reduces the inhibition performed by Bcy1 over Tpk1, and consequently the catalytic activity increases. This positively influences the phosphorylation status of the residue Ser^{179} *in vivo*. These results reinforce the observation that the extent of phosphorylation of Ser^{179} is dependent on Tpk1 catalytic activity.

Role of *tpk1*^{S179A} and *tpk1*^{S179D} mutants on cAMP/PKA pathway-controlled phenotypes

To evaluate the *in vivo* relevance of Tpk1 phosphorylation on Ser^{179}, we analysed several PKA readouts. Phenotypic behaviour analysis was performed by phenotypic comparison of mutant yeast strains expressing Tpk1, *tpk1*^{S179A} and *tpk1*^{S179D} as the sole source of PKA activity (Figure 5). First, we analysed the growth profile on fermentative and respiratory carbon sources of wild-type and mutant strains and we observed that all of the strains showed similar growth kinetics (Supplementary Figure S1B). In order to evaluate whether the mutation on Ser^{179} altered Tpk1 and Bcy1 protein expression levels, we analysed samples derived from crude extracts by Western blotting, and concluded that none of the PKA subunit levels were affected in cells growing exponentially using different carbon sources, even after cells reached quiescence (results not shown). Figure 5(A) shows that the amount of glucose remaining in the medium during culture of the *tpk1*^{S179A} mutant strain was slightly higher than in the case of Tpk1 and *tpk1*^{S179D} strains, indicating less efficiency in glucose metabolism in *tpk1*^{S179A} mutant strain. Since glycogen levels are very sensitive to PKA levels, we assessed the glycogen content of mutants and wild-type strains by iodine staining in cells grown on fermentable (glucose) and respiratory carbon sources (glycerol and ethanol). Mutant strain *tpk1*^{S179D} accumulated less glycogen when compared with mutant strain *tpk1*^{S179A}, whereas wild-type cells presented an intermediate glycogen accumulation levels (Figure 5B). The presence of rapamycin in the culture promoted greater accumulation of glycogen in the three strains, indicating that all three versions of Tpk1 were able to reduce PKA activity by increasing the Tpk1–Bcy1 interaction upon TORC1 (target of rapamycin complex 1) inhibition [35].

High PKA activity correlates with a decrease in heat-stress survival and is a suitable readout to reflect PKA activity. Exponential-phase cultures of Tpk1, *tpk1*^{S179A} and *tpk1*^{S179D} were subjected to heat stress, and cell survival was assayed by spot assay. Figure 5(C) shows that *tpk1*^{S179D} showed a reduction in heat-stress tolerance, suggesting high PKA activity in these mutant cells.

Reduction of cAMP/PKA signalling promotes CLS extension [36,37]. To study the effects of Tpk1 mutation on CLS, wild-type and mutant cells were cultured until reaching stationary phase. Survival was measured by spot assay after cells entered stationary phase (Figure 5D). *tpk1*^{S179D} exhibited a reduction

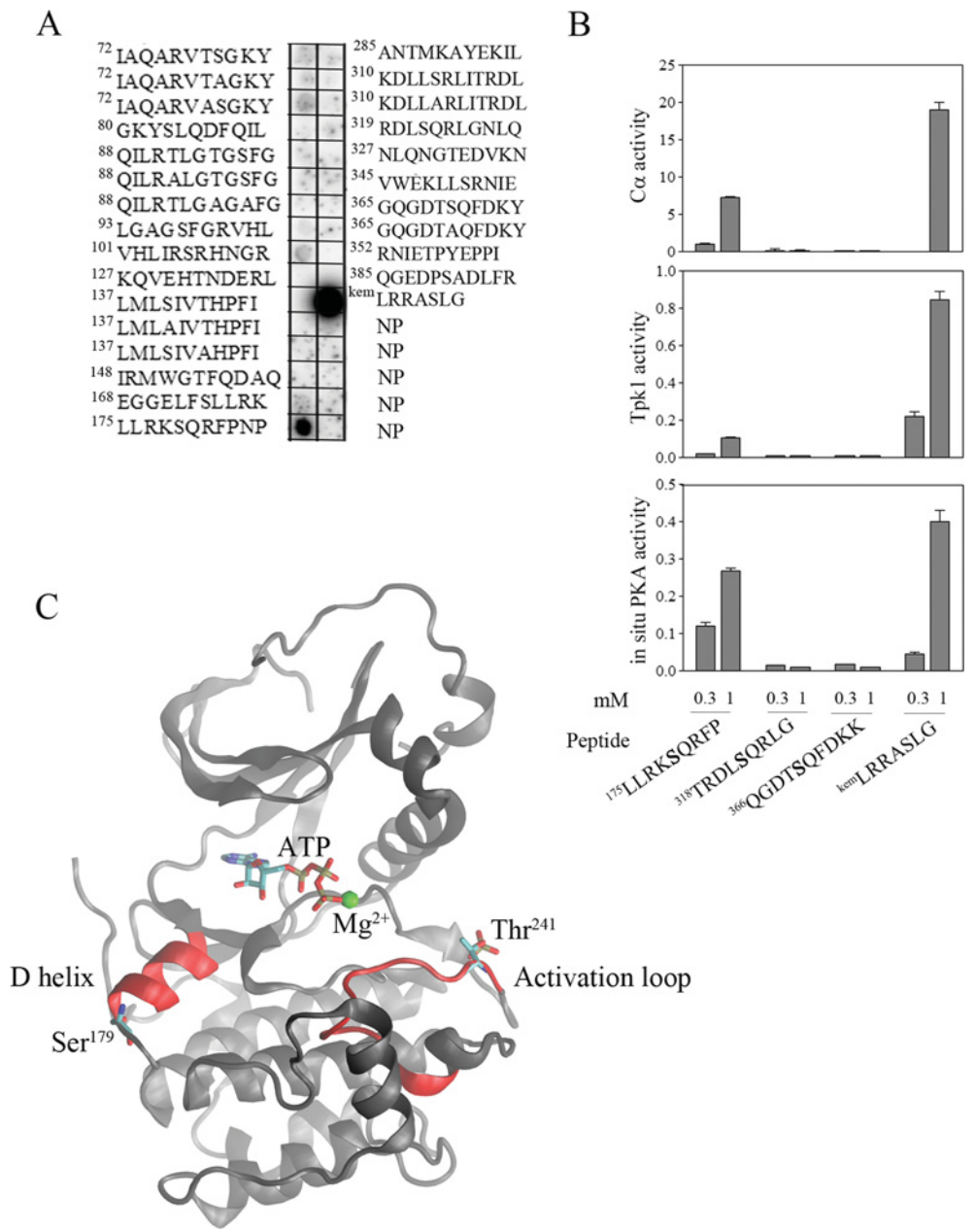

Figure 3 Identification of Ser^{179} target phosphorylation site in Tpk1

(**A**) 11-mer peptides derived from the Tpk1 sequence arrayed on cellulose membrane were incubated with purified Tpk1 as kinase source and radiolabelled with ATP. The sequences of the peptides in each spot are indicated; kem, peptide kemptide; NP, no peptide. A section of the autoradiogram of the peptide array is shown (for the full image, see Supplementary Figure S2 at http://www.biochemj.org/bj/462/bj4620567add.htm). (**B**) *In vitro* and *in situ* PKA kinase assay using 0.3 and 1 mM of the following peptides: L^{175}LRKSQRFP (containing Ser^{179}), T^{318}RDLSQRLG and Q^{366}GDTSQFDKK (as negative controls), kemptide LRRASLG (as positive control), mammalian catalytic subunit Cα or Tpk1 as enzyme source and *TPK1 tpk2*Δ *tpk3*Δ *bcy1*Δ permeabilized cells for the *in situ* assay. *In vitro* kinase activity is expressed as pmol of phosphate incorporated/min and *in situ* kinase activity as pmol of phosphate incorporated/min per 10^6 cells. Results are means $\pm$ S.D. from two independent experiments. (**C**) Ribbon representation of Tpk1 subunit. The protein backbone is presented in grey. Thr^{241} and Ser^{179} and ATP are shown as sticks. Activation loop and D helix are shown in red and the Mg^{2+} ion is shown as a green sphere.

in CLS compared with wild-type cells; conversely, *tpk1*^{S179A} showed an extension of CLS. The results shown in Figure 5 indicate that a phosphomimetic mutation of Ser^{179} to aspartate had as a consequence that cells containing this mutation showed a phenotypic behaviour towards higher PKA activity, whereas cells containing alanine rather than Ser^{179} had a phenotypic behaviour related to a lower PKA activity. Wild-type cells showed a phenotype severity intermediate between the two mutants, suggesting that Ser^{179} is partially phosphorylated *in vivo*.

Taken together, these results are consistent with a model in which Tpk1 phosphorylation on Ser^{179} increases Tpk1 catalytic activity *in vivo*.

Nucleocytoplasmic distribution of Tpk1 is dependent on the negative charge on Ser^{179}

To investigate whether the phosphorylation status of Ser^{179} has an impact on Tpk1 localization, we performed subcellular

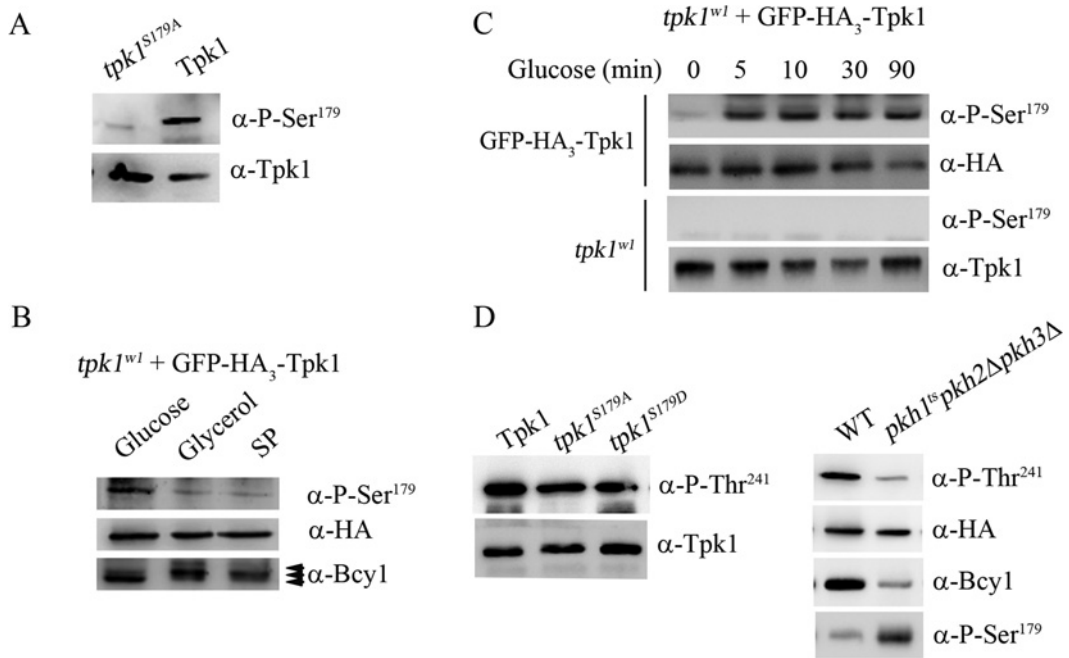

Figure 4 Phosphorylation of Tpk1 on Ser^{179} occurs on active Tpk1 molecules and glucose availability

(**A**) Purified Tpk1 and *tpk1*^{S179A} from glucose-growing cells were subjected to Western blot analysis with anti-pSer^{179}, antibody stripped and further developed with anti-Tpk1 antibody. (**B**) The strain expressing GFP–HA_3–Tpk1 was grown to exponential phase either on glucose or glycerol or to stationary phase. Aliquots containing equal amount of immunopurified GFP–HA_3–Tpk1 were subjected to immunoblot analysis with anti-pSer^{179} antibody. The regulatory subunit associated with each purified GFP–HA_3–Tpk1 was detected by immunoblotting using anti-Bcy1 antibody. The total amount of the catalytic subunit loaded was detected with anti-HA antibody. The arrows indicate Bcy1 isoforms with variable degree of phosphorylation. (**C**) Strain expressing *tpk1*^{w1} + GFP–HA_3–Tpk1 was grown to exponential phase on glycerol (time zero) and subjected to glucose stimulus. At different times (as indicated) equivalent aliquots were taken and GFP–HA_3–Tpk1 was immunopurified with anti-HA antibody (top two rows) and *tpk1*^{w1} was immunopurified with anti-Tpk1 antibody (bottom two rows). Ser^{179} phosphorylation was detected using anti-pSer^{179} antibody and the total amount of catalytic subunits *tpk1*^{w1} or GFP–HA_3–Tpk1 was detected with anti-Tpk1 or anti-HA antibody respectively. (**D**) Left-hand panel: purified Tpk1, *tpk1*^{S179A} or *tpk1*^{S179D} from glucose-growing cells were subjected to Western blot analysis with anti-pThr^{241} antibody, stripped and developed further with anti-Tpk1 antibody. Right-hand panel: wild-type (WT) and *pkh1*^{ts} *pkh2*Δ *pkh3*Δ strains expressing GFP–HA_3–Tpk1 were grown to exponential phase at 24°C and then shifted to 37°C or kept at 24°C as a control for 3 h. GFP–HA_3–Tpk1 was immunopurified from cell extracts and Thr^{241} phosphorylation was analysed by immunoblotting with anti-pThr^{241} antibody. The regulatory subunit associated with purified GFP–HA_3–Tpk1 was detected by immunoblotting with anti-Bcy1 antibody. The total amount of the catalytic subunit loaded was determined by immunoblotting using anti-HA antibody. The phosphorylation status of Ser^{179} was evaluated with anti-pSer^{179} antibody.

localization analysis of Tpk1–GFP, *tpk1*^{S179A}–GFP and *tpk1*^{S179D}–GFP catalytic subunits. As reported previously [18,20], Tpk1–GFP showed a partially nuclear localization during exponential growth on glucose, whereas in glycerol-grown cells its localization was mainly cytoplasmic. However, cells expressing *tpk1*^{S179A}–GFP showed nucleocytoplasmic distribution when grown on either glucose or glycerol (Figure 5E), whereas cells expressing *tpk1*^{S179D}–GFP showed a predominant cytoplasmic localization when grown on both carbon sources. These observations indicate that a negative charge on Ser^{179} of Tpk1 promotes relocalization towards cytoplasm in cells growing on glucose. Since *in vivo* (Figure 5B) and *in vitro* (Figure 6B) results indicate that mutation on Ser^{179} does not affect the Tpk1–Bcy1 interaction, we can rule out that Tpk1 mislocalization in Tpk1 mutants is a consequence of a lack of interaction with Bcy1. We then analysed whether mutation of Ser^{179} had any effect on Bcy1 localization. As shown in Figure 5(E), Bcy1–GFP localization was predominantly nuclear in exponentially glucose-grown cells expressing Tpk1 or *tpk1*^{S179A} subunits. When these cells were cultured in a medium containing glycerol, Bcy1–GFP showed a cytoplasmic localization. However, in the *tpk1*^{S179D} strain, Bcy1–GFP localized in the nucleus when cells were grown either on glucose or on glycerol.

Altogether, these results suggest that cells expressing *tpk1*^{S179D} have enhanced PKA activity by relocalization of Tpk1 towards cytoplasm and nuclear accumulation of Bcy1.

Kinetic characterization of Tpk1 mutant on Ser^{179}

The effect of the negative charge on Ser^{179} on Tpk1 over its kinetic properties was measured by comparing *tpk1*^{S179A} activity with *tpk1*^{S179D} activity using the peptide substrate NTH1-1 [28]. Figure 6(A) shows that *tpk1*^{S179D} has a 25-fold increase in V_{max}, when using the peptide NTH1-1 as a substrate, when compared with *tpk1*^{S179A}. The K_m, however, was not significantly affected by the presence of a negative charge on Ser^{179}. Therefore the specificity (V_{max}/K_m) of *tpk1*^{S179D} for a substrate was significantly higher than that of *tpk1*^{S179A}. We further assessed cAMP-dependence of the holoenzyme activity in the presence of saturating concentrations of kemptide as a substrate. The activation curves shown in Figure 6(B) demonstrate similar $A_{0.5}$ for cAMP, suggesting that the Tpk1–Bcy1 interaction was not affected by the acidic nature of Ser^{179}. These results suggest that a negative charge on Ser^{179} increases the reactivity of Tpk1 towards the substrate.

In order to predict whether there could be a structural correlation to the effect a negative charge on Ser^{179} had on the catalytic activity of Tpk1, we modelled the binding of the NTH1-1 substrate on the catalytic site of the crystal structure of Tpk1. After a multiple alignment using MultiSeq [38] of all of the crystallized complexes of mammalian Cα co-complexed with different ligands, substrates and inhibitors, we chose the bovine PKA catalytic subunit Cα (PDB code 1Q24) structure bound to a

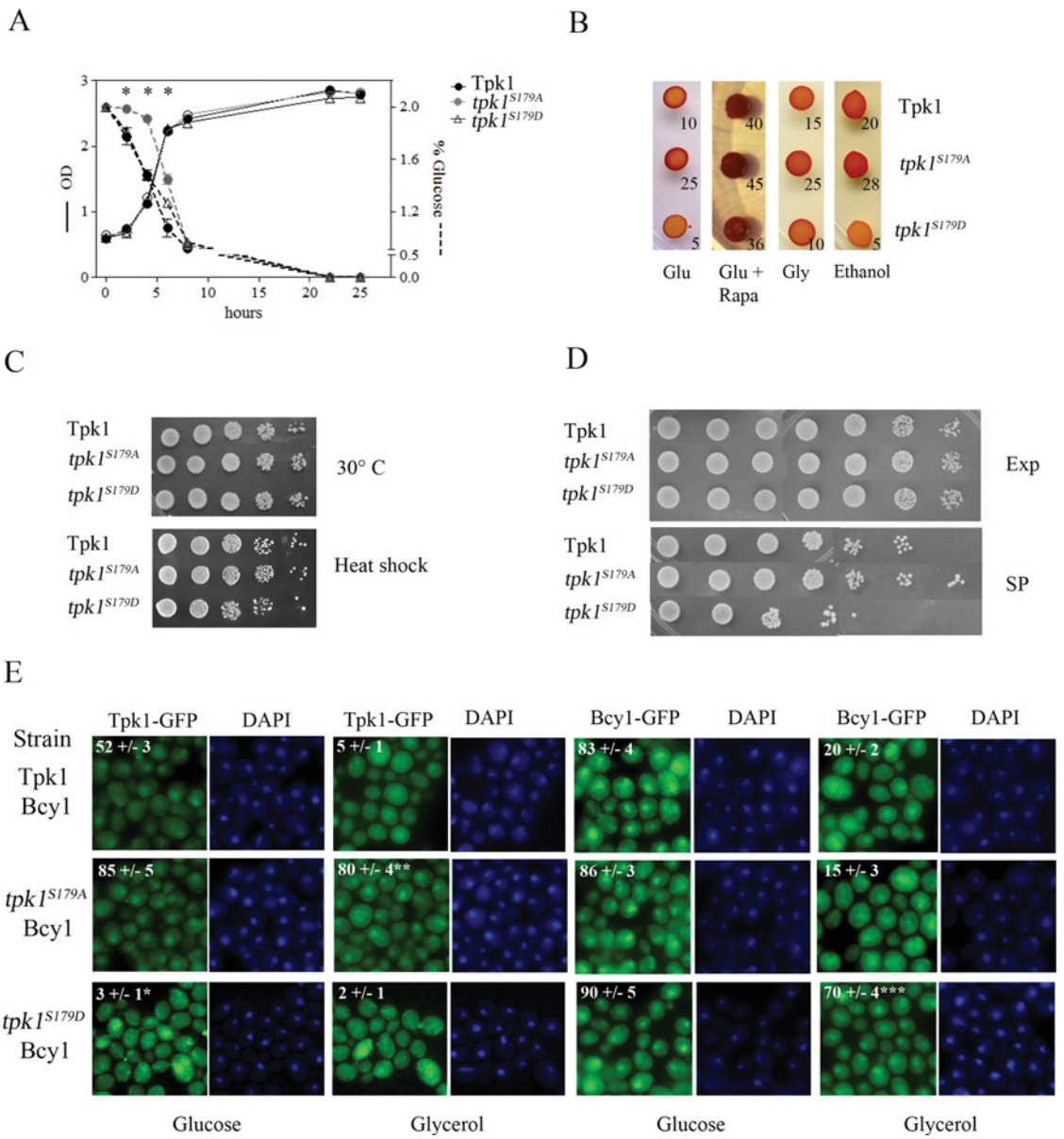

Figure 5 ***In vivo*** **role of negative charge on Ser[179] in Tpk1**

Cells expressing Tpk1, *tpk1*^{S179A} or *tpk1*^{S179D} as the sole kinase source were used for several PKA readouts analyses. (**A**) Growth curve on glucose and glucose consumption during the diauxic shift. Glucose consumption curves show means ± S.D. for three independent cultures. *$P < 0.05$ for *tpk1*^{S179A} compared with Tpk1 and *tpk1*^{S179D} at 2, 4 and 6 h. (**B**) Glycogen accumulation on different carbon sources, tested by iodine staining of culture spotted and grown for 48 h. (Glu, SDGlu plates; Glu + Rapa: SDGlu plates containing 5 ng/ml rapamycin; Gly, SDGly plates; Ethanol, SD-ethanol plates). The numbers under each spot indicates the quantification of iodine staining by densitometric analysis. (**C**) Heat-shock survival analysed by incubation of exponentially growing cells at 54 °C for 8 min, serial dilution by a factor of 10, and growth on SDGlu plates, for 48 h at 30 °C before photography. (**D**) Lifespan of quiescent cells evaluated by spot assay of 12-old-day culture. Viability of exponential cultures was used as control. (**E**) Subcellular localization of Tpk1–GFP, *tpk1*^{S179A}–GFP, *tpk1*^{S179D}–GFP, Tpk1 Bcy1–GFP and *tpk1*^{S179A} Bcy1–GFP, *tpk1*^{S179D} Bcy1–GFP in exponential glucose- and glycerol-growing cells determined by fluorescence microscopy. Nuclei were stained with DAPI. Results are mean ± S.D. percentages of cells with nuclear fluorescence stronger than cytoplasmic fluorescence for three independent cultures. *$P < 0.05$ for Tpk1–GFP compared with *tpk1*^{S179D}–GFP on glucose; **$P < 0.05$ for Tpk1–GFP compared with *tpk1*^{S179A}–GFP on glycerol; ***$P < 0.05$ for Tpk1–Bcy1–GFP compared with *tpk1*^{S179D}–Bcy1–GFP on glycerol.

peptide representing the pseudosubstrate PKI, together with ATP and Mg^{2+} as the best template to model the crystal structure of Tpk1 (PDB code 1FOT) in which we introduced Asp[179] as a phosphomimetic analogue of phosphorylated Ser[179] using FoldX 3.0 [34]. We got a first model of the complex aligning both 1FOT and 1Q24 structures and mutating, by mean of FoldX, the bound peptide to NTH1-1 sequence, to have an approximate peptide docking in the context of the Tpk1 subunit. On bovine PKA Cα structures, there is a displacement of the N-lobe domain respect to the C-lobe domain. This is particularly evident in a C-lobe region close to the ligand-docking site. Therefore, to improve the alignment, we limited it to C-lobe (residues 169–361 for 1FOT and 125–370 for 1Q24). Given that our modelling tool keeps the backbone rigid, the resulting model is an approximation of how our peptide substrate could fit in the context of Tpk1 subunit. In this context, we evaluated residues that could interact with the peptide substrate and found that Asp[179] is quite close to arginine (P-5) on the NTH1-1 peptide [approximately

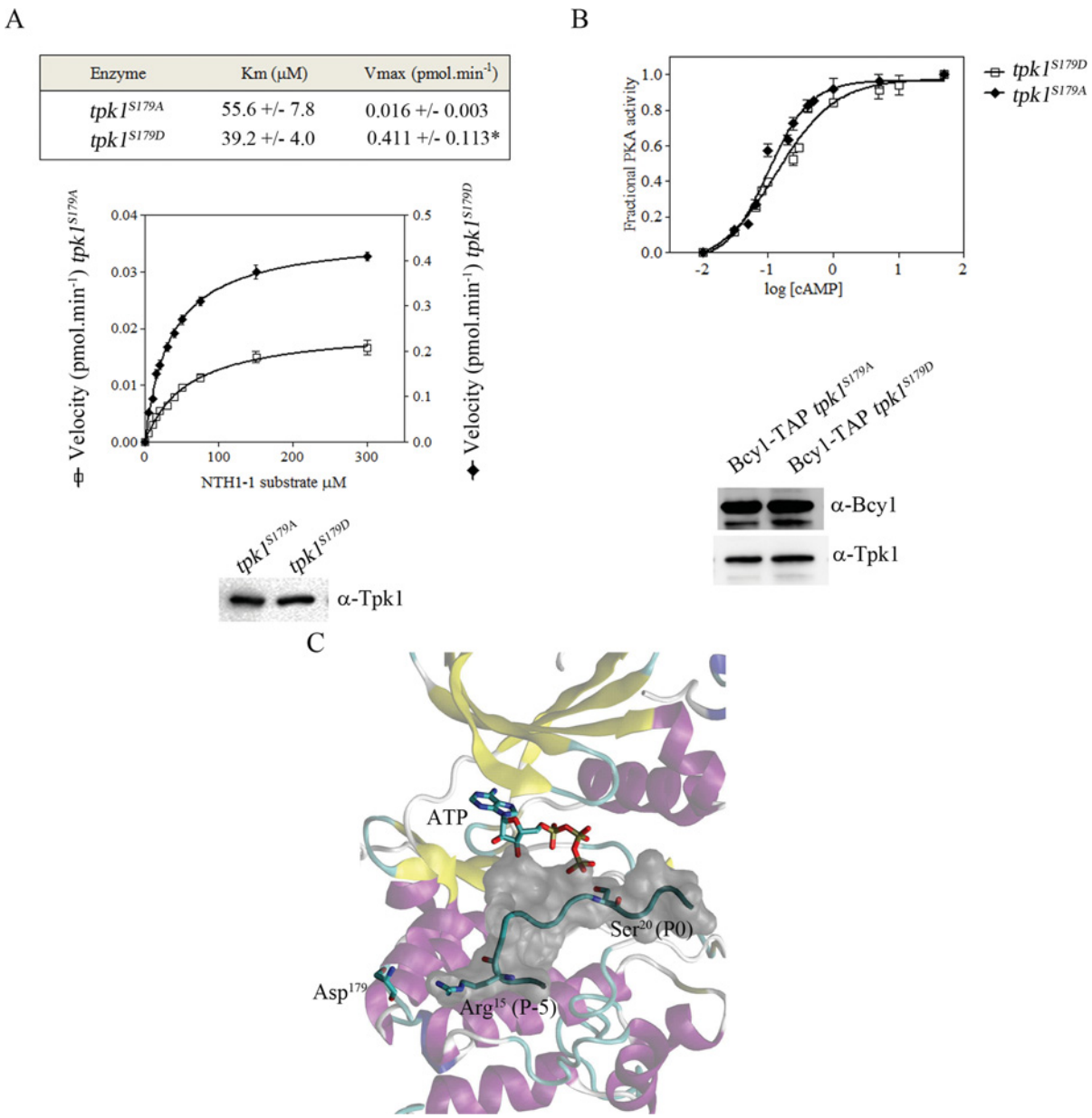

Figure 6 Kinetic parameters of Tpk1, *tpk1*^{S179A} and *tpk1*^{S179D}

(**A**) Purified preparations of catalytic subunit mutant versions *tpk1*^{S179A} and *tpk1*^{S179D} from strains CS-S179A-BTAP or CS-S179D-BTAP were used to determine K_m and relative V_{max} using NTH1-1 synthetic peptide as substrate. Results are means ± S.D. for three independent enzymatic purifications; $^*P < 0.005$. The amount of catalytic subunits used for the assay was quantified by Western blotting using anti-Tpk1 antibody on aliquots of purified *tpk1*^{S179A} and *tpk1*^{S179D} (as shown below). (**B**) *tpk1*^{S179A}–Bcy1 and *tpk1*^{S179D}–Bcy1 purified holoenzymes were obtained from strains CS-S179A-BTAP or CS-S179D-BTAP as described in the Experimental section. An equivalent amount of holoenzymes was incubated with increasing concentrations of cAMP for 10 min at 30 °C with 100 μM [γ-^{32}P]ATP and the peptide NTH1-1 (3-fold the K_m value). Results are means ± S.D. for four independent holoenzyme preparations. PKA activity is represented relative to the activity at 100 μM cAMP taken as 1. The amount of purified holoenzymes used in the assays was quantified by Western blotting with anti-Tpk1 and anti-Bcy1 antibodies on aliquots of enzyme preparations. (**C**) Docking of NTH1-1 to Tpk1 yeast kinase. Close-up of the docking groove highlighting Arg^{15} (P-5) and Ser^{20} (phosphorylatable residue P0) from NTH1-1 peptide and Ser^{179} of Tpk1 as sticks. The bulk of the substrate is depicted as transparent grey. ATP is depicted as sticks.

7 Å (1 Å = 0.1 nm) to the backbone, and 10 Å to the side chain (Figure 6C)]. Given the charges in the residues involved we hypothesize that allowing backbone flexibility (either in a model or in solution), this distance could be reduced improving the interaction. As a support for this prediction, it has been reported that when the natural arginine residue at P-5 of Nth1-1 was replaced by an acidic residue, the peptide showed lower phosphorylation as determined by peptide array phosphorylation assay [28].

DISCUSSION

We have demonstrated previously that cells growing on non-fermentable carbon sources or stationary phase contain less phosphorylated Tpk1 and that, upon stimulation with glucose, the degree of Tpk1 phosphorylation is increased [22].

Our results now suggest that during activation of the cAMP/PKA pathway evoked by glucose, Tpk1 phosphorylation

occurs via an autophosphorylation mechanism (Figure 1). We have characterized Ser[179] as a target site for Tpk1 phosphorylation (Figure 3). Respiring or stationary-phase cells, which display low PKA activity [39], show a reduced phosphorylation state of Ser[179] of Tpk1. After glucose stimulation of the cAMP/PKA pathway, an increase in the phosphorylation state of Ser[179] was observed only on active Tpk1 molecules (Figure 4), suggesting that Ser[179] might be a target residue of Tpk1 autophosphorylation, ruling out the possibility that a PKA-dependent kinase could be responsible for the glucose-dependent phosphorylation on Ser[179] of Tpk1.

The plethora of structural information on mammalian PKA indicates that the role of protein dynamics in the communication of substrate recognition with catalysis is prominent [40], therefore a *cis*-phosphorylation mechanism could be possible. On the other hand, analysis of intermolecular contacts between various crystal forms of different conformational states of mammalian Cα catalytic subunit shows that residues from the catalytic loop of one molecule can interact with residues of the αD helix of another molecule, suggesting that a *trans*-phosphorylation between two C subunits of the same holoenzyme molecule could be possible [41]. However, experiments to elucidate a *trans*- or *cis*-phosphorylation mechanism need to be investigated.

Both mammalian and yeast catalytic subunits are regulated by post-translational modifications, but the molecular mechanism seems to be different.

Recently, a mechanistic model has been proposed whereby mammalian C subunit is assembled into an active molecule. C subunit undergoes two phosphorylations events, the first one is the co-translational *cis*-phosphorylation of Ser[338], and the second is the post-translational *trans*-phosphorylation of Thr[197]. The kinase responsible for the *trans*-phosphorylation of Thr[197] could be the C subunit itself or PDK1 [42,43]. Phosphorylated C subunit is resistant to phosphatases and assembles into an inactive holoenzyme by association with the regulatory subunit. In the presence of high cAMP levels and oxidative stress, the C subunit is sensitive to oxidation of Cys[199] and can subsequently be dephosphorylated by phosphatases [2].

In *S. cerevisiae*, it has been shown that Thr[241] in the Tpk1 activation loop is phosphorylated by Pkh1 immediately after the catalytic subunit is synthesized [5]. Besides Tpk1, an uncharacterized residue on Tpk2 and Thr[242] in Tpk3 are also phosphorylated *in vivo* by Pkh1 with different efficiency. Pkh1 phosphorylation of each Tpk mainly affects the Tpk–Bcy1 interaction [6]. In the present paper, we describe a novel mechanism of regulation of Tpk1 subunit activity by phosphorylation. This post-translational modification is dependent on the nutritional state of the cell marking a difference with Thr[241] phosphorylation that is stable and independent of the carbon source [5].

Importantly, kinetic analysis suggests that phosphorylation of Ser[179] of Tpk1 increases the catalytic efficiency of Tpk1 (Figure 6A), but does not affect the interaction with the regulatory subunit (Figure 6B). Structure modelling shows that a negative charge on an Ser[179] is near to a positive charge on an arginine (P-5) residue on the substrate supporting the results shown in Figure 6(A).

Dephosphorylation of Ser[179] seems not to be a target of glucose-regulated serine/threonine protein phosphatases, PP2A and PP1 [44]; first, we observed that the phosphorylation of Ser[179] increases rapidly, within 5 min of glucose stimulus, and is sustained in cells continuously growing on glucose, and, secondly, the reduction of Ser[179] phosphorylation was observed when cells were grown on glycerol or in stationary-phase cells.

We have observed that the phosphorylation state of Ser[179] does not affect the phosphorylation of Thr[241]. In contrast, reduction of Thr[241] phosphorylation after Pkh1 inactivation increased Ser[179] phosphorylation. This result could be explained taking into account that a reduction in the activation loop Thr[241] phosphorylation reduces the Tpk1–Bcy1 interaction, and, as a consequence, there are more active free Tpk1 molecules and hence higher PKA activity that could promote an increase in the phosphorylation state of Ser[179] of Tpk1.

Sequence alignments between Tpk1, Tpk2 and Tpk3 showed that Ser[179] is conserved in all three Tpk isoforms. However, two-dimensional electrophoresis analysis showed that Tpk1 and Tpk3, but not Tpk2, changed mobility upon glucose stimulus, suggesting that each Tpk isoform could be differentially regulated during the transition from respiratory to fermentative metabolism (results not shown). Mammalian C subunit showed a structurally equivalent residue to Ser[179] of Tpk1, Ser[139], positioned at the beginning of the E-helix. Ser[139] phosphorylation was observed in the recombinant enzyme, but has not been observed in the mammalian enzyme. A mutant version of Ser[139] has not shown any functional consequences on its catalytic activity and on its interaction with its physiological inhibitors [45].

Effect of phosphorylation of Ser[179] of Tpk1 on *in vivo* PKA activity

In *S. cerevisiae*, PKA positively regulates the process associated with rapid fermentative growth, while acting negatively over processes associated with respiratory growth or stationary phase [39]. Extracellular glucose sensing and signalling is mediated by the cAMP/PKA pathway, affecting several downstream targets, thereby allowing cells to make the necessary adaptations for fermentative growth. These include the up-regulation of glycolysis, the stimulation of cell growth and cell cycle progression, the down-regulation of stress resistance and gluconeogenesis, and the mobilization of the reserve carbohydrate glycogen and the stress protector trehalose [17,46–48]. Phenotypic analysis indicated that the acidic charge on Ser[179] of Tpk1 promotes high PKA activity *in vivo* (Figures 5A–5D).

Typically, Tpk1 presents a partially nuclear accumulation during exponential growth, whereas it translocates to cytoplasm under glycerol or stationary phase [18,20]. Tpk1 nuclear accumulation is dependent on Bcy1 interaction, either due to low intracellular cAMP levels [49] or by an increment in the Tpk1–Bcy1 interaction as a consequence of post-translational modifications on Tpk1 [6] or Bcy1 [35]. Subcellular localization analysis showed that an acidic charge on Tpk1 Ser[179] promotes its cytoplasmic localization when cells are grown on glucose, whereas Bcy1 shows a predominantly nuclear accumulation (Figure 5E). Cytoplasmic relocation of *tpk1*^{S179D} seems not to be a result from a lower affinity in the Tpk1–Bcy1 interaction, since both purified *tpk1*^{S179A} and *tpk1*^{S179D} had similar $A_{0.5}$ values for cAMP (Figure 6B). The mechanism by which Ser[179] mutation affects the nucleocytoplasmic distribution needs to be clarified.

The cytoplasmic accumulation of more efficient Tpk1 catalytic subunits could be a mechanism to increase PKA activity. Accordingly, it has been described that Sch9 enhances PKA activity through subcellular redistribution of Bcy1 and Tpk [19].

Therefore the overall results of the present study suggest that during cAMP/PKA pathway stimulation evoked by glucose, Tpk1 increases its phosphorylation state via an autocatalytic mechanism on, at least, Ser[179] of Tpk1. Phosphorylation of Ser[179] of Tpk1 results in a more active Tpk1 catalytic subunit and promotes its cytoplasmic accumulation. Thus glucose-dependent autophosphorylation of Ser[179] of Tpk1 may be a fine-tune regulation of PKA activity by increasing the cytoplasmic level of kinase activity in order to maintain fermentative metabolism.

AUTHOR CONTRIBUTION

Clara Andrea Solari, Marcelo Pugliessi and Vanesa Tudisca designed and performed experiments. Alejandro Daniel Nadra performed structural analysis. Silvia Moreno provided critical insight into data interpretation and contributed to write the paper. Paula Portela designed, performed experiments, analysed data and wrote the paper.

ACKNOWLEDGEMENTS

We are grateful to Dr Thomas Fox for the gift of plasmids and Professor Johan Thevelein for the gift of plasmids and anti-pThr^{241} antibody. We acknowledge the help of Professor Susan Taylor, from the University of California San Diego, San Diego, CA, U.S.A., for the gift of the peptide array.

FUNDING

A.N., S.M. and P.P. are researchers from Consejo Nacional de Investigaciones Científicas y Técnicas (CONICET). This work was supported by a Ph.D. fellowship from Consejo Nacional de Investigaciones Científicas y Técnicas (CONICET) to V.T., and by the Agencia Nacional de Promoción Científica y Tecnológica [grant number PICT 2195], the University of Buenos Aires [grant number UBA X-528] and Consejo Nacional de Investigaciones Científicas y Técnicas (CONICET) [grant number PIP 0519].

REFERENCES

1 Taylor, S. S., Zhang, P., Steichen, J. M., Keshwani, M. M. and Kornev, A. P. (2013) PKA: lessons learned after twenty years. Biochim. Biophys. Acta **1834**, 1271–1278 CrossRef PubMed

2 Keshwani, M. M., Klammt, C., von Daake, S., Ma, Y., Kornev, A. P., Choe, S., Insel, P. A. and Taylor, S. S. (2012) Cotranslational *cis*-phosphorylation of the COOH-terminal tail is a key priming step in the maturation of cAMP-dependent protein kinase. Proc. Natl. Acad. Sci. U.S.A. **109**, 1221–1229 CrossRef

3 Cheng, X., Ma, Y., Moore, M., Hemmings, B. A. and Taylor, S. S. (1998) Phosphorylation and activation of cAMP-dependent protein kinase by phosphoinositide-dependent protein kinase. Proc. Natl. Acad. Sci. U.S.A. **95**, 9849–9854 CrossRef PubMed

4 Williams, M. R., Arthur, J. S., Balendran, A., van der Kaay, J., Poli, V., Cohen, P. and Alessi, D. R. (2000) The role of 3-phosphoinositide-dependent protein kinase 1 in activating AGC kinases defined in embryonic stem cells. Curr. Biol. **10**, 439–448 CrossRef PubMed

5 Voordeckers, K., Kimpe, M., Haesendonckx, S., Louwet, W., Versele, M. and Thevelein, J. M. (2011) Yeast 3-phosphoinositide-dependent protein kinase-1 (PDK1) orthologs Pkh1–3 differentially regulate phosphorylation of protein kinase A (PKA) and the protein kinase B (PKB)/S6K ortholog Sch9. J. Biol. Chem. **286**, 22017–22027 CrossRef PubMed

6 Haesendonckx, S., Tudisca, V., Voordeckers, K., Moreno, S., Thevelein, J. M. and Portela, P. (2012) The activation loop of PKA catalytic isoforms is differentially phosphorylated by Pkh protein kinases in *Saccharomyces cerevisiae*. Biochem. J. **448**, 307–320 CrossRef PubMed

7 Thevelein, J. M. (1991) Fermentable sugars and intracellular acidification as specific activators of the RAS–adenylate cyclase signalling pathway in yeast: the relationship to nutrient-induced cell cycle control. Mol. Microbiol. **5**, 1301–1307 CrossRef PubMed

8 Rolland, F., De Winde, J. H., Lemaire, K., Boles, E., Thevelein, J. M. and Winderickx, J. (2000) Glucose-induced cAMP signalling in yeast requires both a G-protein coupled receptor system for extracellular glucose detection and a separable hexose kinase-dependent sensing process. Mol. Microbiol. **38**, 348–358 CrossRef PubMed

9 Lu, A. and Hirsch, J. P. (2005) Cyclic AMP-independent regulation of protein kinase A substrate phosphorylation by Kelch repeat proteins. Eukaryot. Cell **4**, 1794–1800 CrossRef PubMed

10 Peeters, T., Louwet, W., Gelade, R., Nauwelaers, D., Thevelein, J. M. and Versele, M. (2006) Kelch-repeat proteins interacting with the Gα protein Gpa2 bypass adenylate cyclase for direct regulation of protein kinase A in yeast. Proc. Natl. Acad. Sci. U.S.A. **103**, 13034–13039 CrossRef PubMed

11 Budhwar, R., Lu, A. and Hirsch, J. P. (2010) Nutrient control of yeast PKA activity involves opposing effects on phosphorylation of the Bcy1 regulatory subunit. Mol. Biol. Cell **21**, 3749–3758 CrossRef PubMed

12 Budhwar, R., Fang, G. and Hirsch, J. P. (2011) Kelch repeat proteins control yeast PKA activity in response to nutrient availability. Cell Cycle **10**, 767–770 CrossRef PubMed

13 Ma, P., Wera, S., Van Dijck, P. and Thevelein, J. M. (1999) The PDE1-encoded low-affinity phosphodiesterase in the yeast *Saccharomyces cerevisiae* has a specific function in controlling agonist-induced cAMP signaling. Mol. Biol. Cell **10**, 91–104 CrossRef PubMed

14 Hu, Y., Liu, E., Bai, X. and Zhang, A. (2010) The localization and concentration of the PDE2-encoded high-affinity cAMP phosphodiesterase is regulated by cAMP-dependent protein kinase A in the yeast *Saccharomyces cerevisiae*. FEMS Yeast Res. **10**, 177–187 CrossRef PubMed

15 Durnez, P., Pernambuco, M. B., Oris, E., Arguelles, J. C., Mergelsberg, H. and Thevelein, J. M. (1994) Activation of trehalase during growth induction by nitrogen sources in the yeast *Saccharomyces cerevisiae* depends on the free catalytic subunits of cAMP-dependent protein kinase, but not on functional Ras proteins. Yeast **10**, 1049–1064 CrossRef PubMed

16 Thevelein, J. M., Bonini, B. M., Castermans, D., Haesendonckx, S., Kriel, J., Louwet, W., Thayumanavan, P., Popova, Y., Rubio-Texeira, M., Schepers, W. et al. (2008) Novel mechanisms in nutrient activation of the yeast protein kinase A pathway. Acta Microbiol. Immunol. Hung. **55**, 75–89 CrossRef PubMed

17 Thevelein, J. M., Cauwenberg, L., Colombo, S., De Winde, J. H., Donation, M., Dumortier, F., Kraakman, L., Lemaire, K., Ma, P., Nauwelaers, D. et al. (2000) Nutrient-induced signal transduction through the protein kinase A pathway and its role in the control of metabolism, stress resistance, and growth in yeast. Enzyme Microb. Technol. **26**, 819–825 CrossRef PubMed

18 Griffioen, G., Anghileri, P., Imre, E., Baroni, M. D. and Ruis, H. (2000) Nutritional control of nucleocytoplasmic localization of cAMP-dependent protein kinase catalytic and regulatory subunits in *Saccharomyces cerevisiae*. J. Biol. Chem. **275**, 1449–1456 CrossRef PubMed

19 Zhang, A., Shen, Y., Gao, W. and Dong, J. (2011) Role of Sch9 in regulating Ras–cAMP signal pathway in *Saccharomyces cerevisiae*. FEBS Lett. **585**, 3026–3032 CrossRef PubMed

20 Tudisca, V., Recouvreux, V., Moreno, S., Boy-Marcotte, E., Jacquet, M. and Portela, P. (2010) Differential localization to cytoplasm, nucleus or P-bodies of yeast PKA subunits under different growth conditions. Eur. J. Cell Biol. **89**, 339–348 CrossRef PubMed

21 Tudisca, V., Simpson, C., Castelli, L., Lui, J., Hoyle, N., Moreno, S., Ashe, M. and Portela, P. (2012) PKA isoforms coordinate mRNA fate during nutrient starvation. J. Cell Sci. **125**, 5221–5232 CrossRef PubMed

22 Portela, P. and Moreno, S. (2006) Glucose-dependent activation of protein kinase A activity in *Saccharomyces cerevisiae* and phosphorylation of its TPK1 catalytic subunit. Cell. Signal. **18**, 1072–1086 CrossRef PubMed

23 Ito, H., Fukuda, Y., Murata, K. and Kimura, A. (1983) Transformation of intact yeast cells treated with alkali cations. J. Bacteriol. **153**, 163–168 PubMed

24 Muhlrad, D., Hunter, R. and Parker, R. (1992) A rapid method for localized mutagenesis of yeast genes. Yeast **8**, 79–82 CrossRef PubMed

25 Huh, W. K., Falvo, J. V., Gerke, L. C., Carroll, A. S., Howson, R. W., Weissman, J. S. and O'Shea, E. K. (2003) Global analysis of protein localization in budding yeast. Nature **425**, 686–691 CrossRef PubMed

26 Portela, P., Howell, S., Moreno, S. and Rossi, S. (2002) *In vivo* and *in vitro* phosphorylation of two isoforms of yeast pyruvate kinase by protein kinase A. J. Biol. Chem. **277**, 30477–30487 CrossRef PubMed

27 Puig, O., Caspary, F., Rigaut, G., Rutz, B., Bouveret, E., Bragado-Nilsson, E., Wilm, M. and Seraphin, B. (2001) The tandem affinity purification (TAP) method: a general procedure of protein complex purification. Methods **24**, 218–229 CrossRef PubMed

28 Galello, F., Portela, P., Moreno, S. and Rossi, S. (2010) Characterization of substrates that have a differential effect on *Saccharomyces cerevisiae* protein kinase A holoenzyme activation. J. Biol. Chem. **285**, 29770–29779 CrossRef PubMed

29 Roskoski, Jr, R. (1983) Assays of protein kinase. Methods Enzymol. **99**, 3–6 CrossRef PubMed

30 Chester, V. E. (1968) Heritable glycogen-storage deficiency in yeast and its induction by ultra-violet light. J. Gen. Microbiol. **51**, 49–56 CrossRef PubMed

31 Mirisola, M. G., Braun, R. J. and Petranovic, D. (2013) Approaches to study yeast cell aging and death. FEMS Yeast Res., doi:10.1111/1567-1364.12112

32 Thevelein, J. M., Beullens, M., Honshoven, F., Hoebeeck, G., Detremerie, K., Griewel, B., den Hollander, J. A. and Jans, A. W. (1987) Regulation of the cAMP level in the yeast *Saccharomyces cerevisiae*: the glucose-induced cAMP signal is not mediated by a transient drop in the intracellular pH. J. Gen. Microbiol. **133**, 2197–2205 PubMed

33 Gibbs, C. S., Knighton, D. R., Sowadski, J. M., Taylor, S. S. and Zoller, M. J. (1992) Systematic mutational analysis of cAMP-dependent protein kinase identifies unregulated catalytic subunits and defines regions important for the recognition of the regulatory subunit. J. Biol. Chem. **267**, 4806–4814 PubMed

34 Schymkowitz, J., Borg, J., Stricher, F., Nys, R., Rousseau, F. and Serrano, L. (2005) The FoldX web server: an online force field. Nucleic Acids Res. **33**, W382–W388 CrossRef PubMed

35 Soulard, A., Cremonesi, A., Moes, S., Schutz, F., Jeno, P. and Hall, M. N. (2010) The rapamycin-sensitive phosphoproteome reveals that TOR controls protein kinase A toward some but not all substrates. Mol. Biol. Cell **21**, 3475–3486 CrossRef PubMed

36 Fabrizio, P., Pozza, F., Pletcher, S. D., Gendron, C. M. and Longo, V. D. (2001) Regulation of longevity and stress resistance by Sch9 in yeast. Science **292**, 288–290 CrossRef PubMed

37 Longo, V. D. and Fabrizio, P. (2012) Chronological aging in *Saccharomyces cerevisiae*. Subcell. Biochem. **57**, 101–121 CrossRef PubMed
38 Roberts, E., Eargle, J., Wright, D. and Luthey-Schulten, Z. (2006) MultiSeq: unifying sequence and structure data for evolutionary analysis. BMC Bioinformatics **7**, 382 CrossRef PubMed
39 Thevelein, J. M. and de Winde, J. H. (1999) Novel sensing mechanisms and targets for the cAMP-protein kinase A pathway in the yeast *Saccharomyces cerevisiae*. Mol. Microbiol. **33**, 904–918 CrossRef PubMed
40 Masterson, L. R., Cheng, C., Yu, T., Tonelli, M., Kornev, A., Taylor, S. S. and Veglia, G. (2010) Dynamics connect substrate recognition to catalysis in protein kinase A. Nat. Chem. Biol. **6**, 821–828 CrossRef PubMed
41 Karlsson, R., Madhusudan, Taylor, S. S. and Sowadski, J. M. (1994) Intermolecular contacts in various crystal forms related to the open and closed conformational states of the catalytic subunit of cAMP-dependent protein kinase. Acta Crystallogr. D Biol. Crystallogr. **50**, 657–662 CrossRef PubMed
42 Nirula, A., Ho, M., Phee, H., Roose, J. and Weiss, A. (2006) Phosphoinositide-dependent kinase 1 targets protein kinase A in a pathway that regulates interleukin 4. J. Exp. Med. **203**, 1733–1744 CrossRef PubMed
43 Cauthron, R. D., Carter, K. B., Liauw, S. and Steinberg, R. A. (1998) Physiological phosphorylation of protein kinase A at Thr-197 is by a protein kinase A kinase. Mol. Cell. Biol. **18**, 1416–1423 PubMed
44 Castermans, D., Somers, I., Kriel, J., Louwet, W., Wera, S., Versele, M., Janssens, V. and Thevelein, J. M. (2012) Glucose-induced posttranslational activation of protein phosphatases PP2A and PP1 in yeast. Cell Res. **22**, 1058–1077 CrossRef PubMed
45 Yonemoto, W., McGlone, M. L., Grant, B. and Taylor, S. S. (1997) Autophosphorylation of the catalytic subunit of cAMP-dependent protein kinase in *Escherichia coli*. Protein Eng. **10**, 915–925 CrossRef PubMed
46 Santangelo, G. M. (2006) Glucose signaling in *Saccharomyces cerevisiae*. Microbiol. Mol. Biol. Rev. **70**, 253–282 CrossRef PubMed
47 Tamaki, H. (2007) Glucose-stimulated cAMP–protein kinase A pathway in yeast *Saccharomyces cerevisiae*. J. Biosci. Bioeng. **104**, 245–250 CrossRef PubMed
48 Gancedo, J. M. (2008) The early steps of glucose signalling in yeast. FEMS Microbiol. Rev. **32**, 673–704 CrossRef PubMed
49 Griffioen, G., Branduardi, P., Ballarini, A., Anghileri, P., Norbeck, J., Baroni, M. D. and Ruis, H. (2001) Nucleocytoplasmic distribution of budding yeast protein kinase A regulatory subunit Bcy1 requires Zds1 and is regulated by Yak1-dependent phosphorylation of its targeting domain. Mol. Cell. Biol. **21**, 511–523 CrossRef PubMed

Received 5 May 2014/16 June 2014; accepted 20 June 2014
Published as BJ Immediate Publication 20 June 2014, doi:10.1042/BJ20140577

Biochem. J. (2014) **462**, 567–579 (Printed in Great Britain) doi:10.1042/BJ20140577

online data

SUPPLEMENTARY ONLINE DATA

Regulation of PKA activity by an autophosphorylation mechanism in *Saccharomyces cerevisiae*

Clara Andrea SOLARI*, Vanesa TUDISCA*, Marcelo PUGLIESSI*, Alejandro Daniel NADRA*, Silvia MORENO* and Paula PORTELA*[1]

*Instituto de Química Biológica, Facultad de Ciencias Exactas y Naturales (IQUIBICEN-CONICET), Universidad de Buenos Aires, Buenos Aires, Argentina

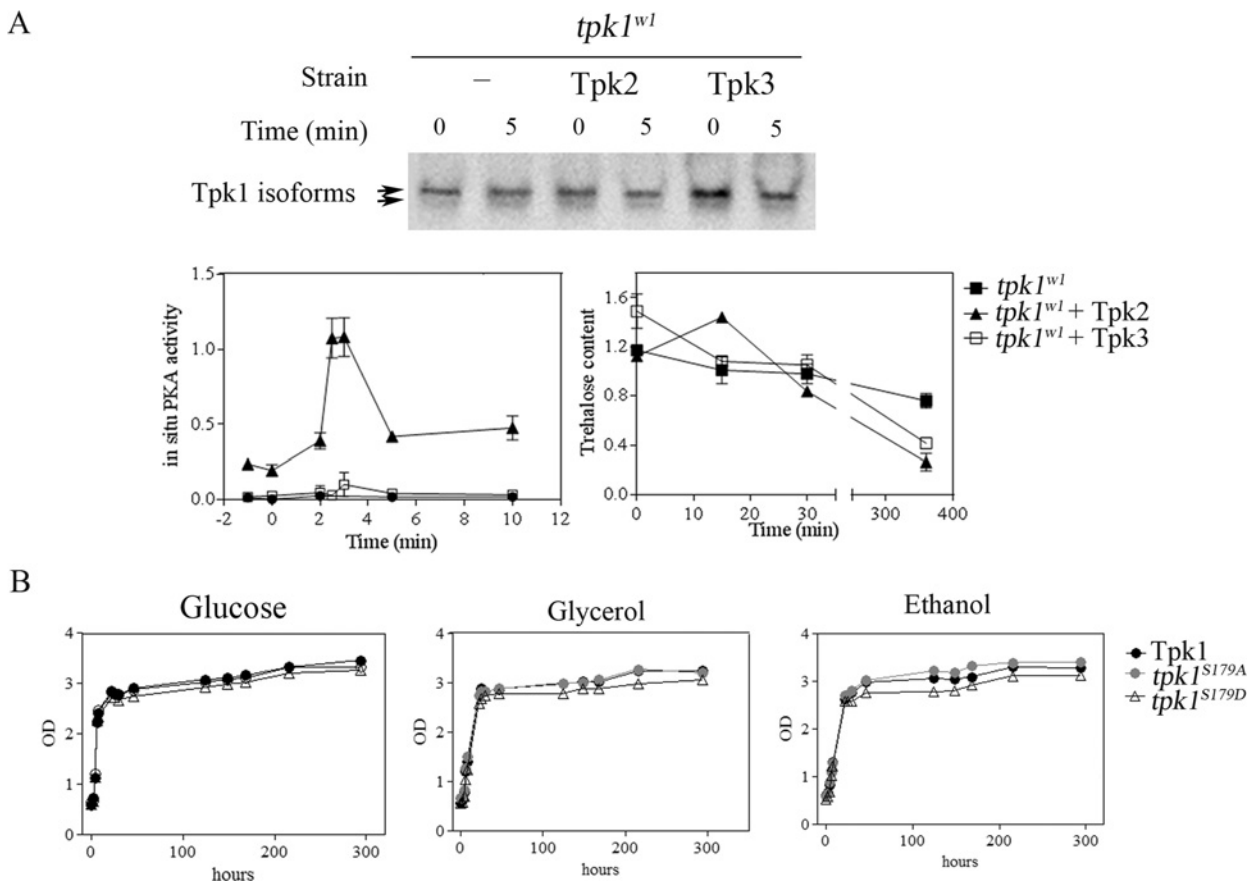

Figure S1 Analysis of glucose-induced phosphorylation dependence of inactive *tpk1*^{d} on Tpk2 and Tpk3 activity

(**A**) Upper panel: *tpk1*^{w1} + Tpk2 and *tpk1*^{w1} + Tpk3 strains were grown on SD containing 2 % glycerol to exponential phase. Samples were taken before (0 min) and after (5 min) addition of 100 mM glucose. Proteins in crude extracts were separated by native gel electrophoresis and Tpk1 isoforms were developed using anti-Tpk1 antibody. Black arrows indicate respectively higher and lower Tpk1 isoform. Lower panels: *in situ* PKA activity measured in permeabilized cells (left) and trehalose levels (right) measured at different times after 100 mM glucose addition. Results are means±S.D. from three independent experiments. (**B**) Growth kinetics on glucose, glycerol and ethanol of Tpk1, *tpk1*^{S179A} and *tpk1*^{S179D}.

[1] To whom correspondence should be addressed (email pportela@qb.fcen.uba.ar).

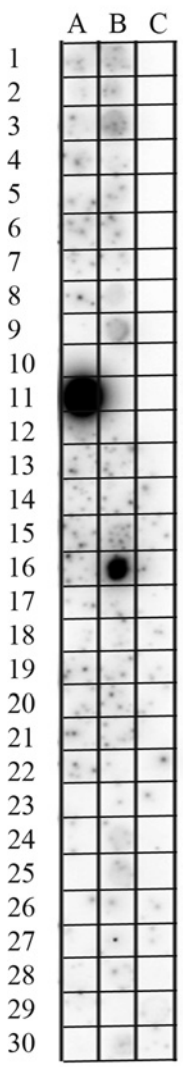

Position	Peptide sequence
C13	[1]MSTEEQNGGGQ[11]
C14	[1]MATEEQNGGGQ[11]
C15	[1]MSAEEQNGGGQ[11]
C16	[8]GGGQKSLDDRGQ[19]
C17	[16]DRQGEESQKGE[26]
C18	[23]QKGETSERE[31]
C19	[23]QKGETAERE[31]
C20	[23]QKGEASERE[31]
C21	[29]ERETTATESGNE[40]
C22	[29]EREATATESGNE[40]
C23	[29]ERETAATESGNE[40]
C24	[29]ERETTAAESGNE[40]
C25	[29]ERETTATEAGNE[40]
C26	[38]GNESKSVEKEG[48]
C27	[38]GNEAKSVEKEG[48]
C28	[38]GNESKAVEKEG[48]
C29	[46]KEGGETQEKPK[56]
C30	[56]KQPHVTYYNEE[66]
B1	[72]IAQARVTSGKY[82]
B2	[72]IAQARVTAGKY[82]
B3	[72]IAQARVASGKY[82]
B4	[80]GKYSLQDFQIL[90]
B5	[88]QILRTLGTGSFG[99]
B6	[88]QILRALGTGSFG[99]
B7	[88]QILRTLGAGAFG[99]
B8	[93]LGAGSFGRVHL[103]
B9	[101]VHLIRSRHNGR[111]
B10	[127]KQVEHTNDERL[137]
B11	[137]LMLSIVTHPFI[147]
B12	[137]LMLAIVTHPFI[147]
B13	[137]LMLSIVAHPFI[147]
B14	[148]IRMWGTFQDAQ[158]
B15	[168]EGGELFSLLRK[178]
B16	[175]LLRKSQRFPNP[185]
B17	[197]ALEYLHSKDII[207]
B18	[222]GHIKITDFGFA[232]
B19	[234]YVPDVTYTLCG[244]
B20	[234]YVPDVTYALCG[244]
B21	[234]YVPDVTYTpLCG[244]
B22	[234]YVPDVAYTLCG[244]
B23	[242]LCGTPDYIAPE[252]
B24	[251]PEVVSTKPYNK[261]
B25	[251]PEVVATKPYNK[261]
B26	[258]PYNKSIDWWSFGIL[271]
B27	[274]EMLAGYTPFYD[284]
B28	[281]PFYDSNTMK[289]
B29	[281]PFYDANTMK[289]
B30	[285]ANTMKTYEKIL[295]
A1	[285]ANTMKAYEKIL[295]
A2	[310]KDLLSRLITRDL[321]
A3	[310]KDLLARLITRDL[321]
A4	[319]RDLSQRLGNLQ[329]
A5	[327]NLQNGTEDVKN[337]
A6	[345]VWEKLLSRNIE[355]
A7	[365]GQGDTSQFDKY[375]
A8	[365]GQGDTAQFDKY[375]
A9	[352]RNIETPYEPPI[362]
A10	[385]QGEDPSADLFR[395]
A11	LRRASLG
C1-C12	non peptide
A12-A30	non peptide

Figure S2 Peptide array scanning

11–12-mer residue peptides representing all serine or threonine residues in the primary sequence of Tpk1. The putative phosphorylatable amino acid is in the middle of the peptide sequence. For peptides containing more than one phosphorylatable amino acid (underlined on the peptide sequence), an additional version with replacement of each of these amino acids with alanine was included. The phosphorylation reaction was performed as described in the Experimental section of the main text.

Table S1 List of strains and nomenclature used in the present study

Strain name	Genotype	Nomenclature in the Figures	Source
W303-1A	*Mat a leu2 his3 trp1 ade2 can1-100 ura3 GAL SUC*	W303	Thevelein laboratory [1]
S330	W303-1 A *tpk3::tpk1::KanMx4*		Irniger laboratory [2]
YMR 60	W303-1A *tpk1::URA3*	*tpk1*Δ	Thevelein laboratory [1]
YMR 60 + Tpk1	W303-1A *tpk1::URA3* + pTD45-Tpk1	*tpk1*Δ + Tpk1	
YMR 60 + *tpk1*^{d}	W303 1A *tpk1::URA3* + pTD53-*tpk1*^{d}	*tpk1*Δ + *tpk1*^{d}	
S18-1D	*Matα leu2 ura3 his3 trp1 ade8 tpk1*^{w1} *tpk2::HIS3 tpk3::TRP1*	*tpk1*^{w1}	Thevelein laboratory [1]
S18-1D + GFP-HA-Tpk1	S18-1D + Ycp50-GFP-HA$_3$-Tpk1	*tpk1*^{w1} + GFP–HA$_3$–Tpk1	
S18-1D + Tpk2	S18-1D + pTD46-Tpk2	*tpk1*^{w1} + Tpk2	
S18-1D + Tpk3	S18-1D + pTD49-Tpk3	*tpk1*^{w1} + Tpk3	
CS-S179	W303 1A *tpk3::tpk1::KanMx4 tpk2::URA3* + pTD45-Tpk1	Tpk1	The present study
CS-S179A	W303 1A *tpk3::tpk1::KanMx4 tpk2::URA3* + pTD45-*tpk1*^{S179A}	*tpk1*^{S179A}	The present study
CS-S179D	W303 1A *tpk3::tpk1::KanMx4 tpk2::URA3* + pTD45-*tpk1*^{S179D}	*tpk1*^{S179D}	The present study
CS-S179-BTAP	W303 1A *tpk3::tpk1::KanMx4 tpk2::URA3 BCY1-TAP-HIS3* + pTD45-Tpk1	Tpk1 Bcy1–TAP	The present study
CS-S179A-BTAP	W303 1A *tpk3::tpk1::KanMx4 tpk2::URA3 BCY1-TAP-HIS3* + pTD45-*tpk1*^{S179A}	*tpk1*^{S179A} Bcy1–TAP	The present study
CS-S179D-BTAP	W303 1A *tpk3::tpk1::KanMx4 tpk2::URA3 BCY1-TAP-HIS3* + pTD45-*tpk1*^{S179D}	*tpk1*^{S179D} Bcy1–TAP	The present study
YJL164c	BY4741 *Mat a his3 leu2 met15 ura3 TPK1::KanMx4*	*tpk1*Δ	Euroscarf
YJL164c	BY4741 *Mat a his3 leu2 met15 ura3 TPK1::KanMx4* + pTD45-Tpk1-GFP	Tpk1–GFP	
YJL164c	BY4741 *Mat a his3 leu2 met15 ura3 TPK1::KanMx4* + pTD45-*tpk1*^{S179A}-GFP	*tpk1*^{S179A}–GFP	
YJL164c	BY4741 *Mat a his3 leu2 met15 ura3 TPK1::KanMx4* + pTD45-*tpk1*^{S179D}-GFP	*tpk1*^{S179D}–GFP	
CS-S179-BGFP	W303 1A *tpk3::tpk1::KanMx4 tpk2::URA3 BCY1-GFP-HIS3* + pTD45-Tpk1	Tpk1 Bcy1–GFP	The present study
CS-S179A-BGFP	W303 1A *tpk3::tpk1::KanMx4 tpk2::URA3 BCY1-GFP-HIS3* + pTD45-*tpk1* ^{S179A}	*tpk1*^{S179A} Bcy1–GFP	The present study
CS-S179D-BGFP	W303 1A *tpk3::tpk1::KanMx4 tpk2::URA3 BCY1-GFP-HIS3* + pTD45-*tpk1* ^{S179D}	*tpk1*^{S179D} Bcy1–GFP	The present study
S288C TPK1-TAP	*Mat a his3*Δ*1 leu2*Δ*0 met15*Δ*0 ura3*Δ*0 TPK1-TAP-HIS3*	Tpk1–TAP	Open Biosynthesis
S288C TPK1-GFP	*Mat a his3*Δ*1 leu2*Δ*0 met15*Δ*0 ura3*Δ*0 TPK1-GFP-HIS3*	Tpk1–GFP	Invitrogen
S288C BCY1-GFP	*Mat a his3*Δ*1 leu2*Δ*0 met15*Δ*0 ura3*Δ*0 BCY1-GFP-HIS3*	Bcy1–GFP	Invitrogen
YMR 60 + tpk1^{d}	W303 1A *tpk1::URA3* + pTD53-*tpk1*^{d}-TAP	*tpk1*^{d}–TAP	
Tpk1bcy1Δ	*Matα his3 leu2 ura3 trp1 ade8 tpk2::HIS3 tpk3::TRP1 bcy1::LEU2*	Tpk1 *bcy1*Δ	Thevelein laboratory [1]
pkh1^{ts}pkh2Δpkh3Δ	15 Dau *pkh1::PKH1*^{D398G} *pkh2::LEU2 pkh3::KanMX*	*pkh1*^{ts}*pkh2*Δ*pkh3*Δ	Thevelein laboratory [1]
15 Dau	*MAT a leu2 ura3 trp1 his2 ade1*	WT	Matsumoto laboratory [3]

Table S2 Plasmids used in the present study

Plasmid name	Genotype	Source
pTD45-Tpk1	*LEU2*, *TPK1 prom-TPK1*	Fox laboratory
pTD53-*tpk1*^{d}	*LEU2*, *TPK1 prom-tpk1*^{K116R}	Fox laboratory
pTD53-*tpk1*^{d}-TAP	*LEU2*, *TPK1 prom-tpk1*^{K116R}*-TAP-HIS3*	The present study
GFP-HA$_3$-Tpk1	*URA3, ADH1-GFP-HA$_3$-Tpk1*	Thevelein laboratory
pTD46-Tpk2	*LEU2*, *TPK2 prom-TPK2*	Fox laboratory
pTD49-Tpk3	*URA3*, *TPK3 prom-TPK3*	Fox laboratory
pTD45-*tpk1*^{S179A}	*LEU2*, *TPK1 prom- tpk1*^{S179A}	The present study
pTD45-*tpk1*^{S179D}	*LEU2*, *TPK1 prom- tpk1*^{S179D}	The present study
pTD45-Tpk1-GFP	*LEU2*, *TPK1 prom-TPK1-GFP-HIS3*	The present study
pTD45-*tpk1*^{S179D}-GFP	*LEU2*, *TPK1 prom- tpk1*^{S179D}*-GFP-HIS3*	The present study
pTD45-*tpk1*^{S179A}-GFP	*LEU2*, *TPK1 prom- tpk1*^{S179A}*-GFP-HIS3*	The present study

REFERENCES

1 Voordeckers, K., Kimpe, M., Haesendonckx, S., Louwet, W., Versele, M. and Thevelein, J. M. (2011) Yeast 3-phosphoinositide-dependent protein kinase-1 (PDK1) orthologs Pkh1-3 differentially regulate phosphorylation of protein kinase A (PKA) and the protein kinase B (PKB)/S6K ortholog Sch9. J. Biol. Chem. **286**, 22017–22027 CrossRef PubMed

2 Bolte, M., Dieckhoff, P., Krause, C., Braus, G.H. and Irniger, S. (2003) Synergistic inhibition of APC/C by glucose and activated Ras proteins can be mediated by each of the Tpk1-3 proteins in Saccharomyces cerevisiae. Microbiology. **149**, 1205–1216 CrossRef PubMed

3 Inagaki, M., Schmelzle, T., Yamaguchi, K., Irie, K., Hall, M. N. and Matsumoto, K. (1999) PDK1 homologs activate the Pkc1-mitogen-activated protein kinase pathway in yeast. Mol. Cell. Biol. **19**, 8344–8352 PubMed

Received 5 May 2014/16 June 2014; accepted 20 June 2014
Published as BJ Immediate Publication 20 June 2014, doi:10.1042/BJ20140577